Genetic Developmental Timing Revealed by Inter-Species Transplantations in Fish.

Jana Franziska Fuhrmann[1,3], Lorena Buono[2], Leonie Adelmann[1], Juan Ramón Martinez Morales[2], Lázaro Centanin[1]

1 Lab of Clonal Analysis, Center for Organismal Studies, Universität Heidelberg, INF230, 69120 Heidelberg, Germany

2 Centro Andaluz de Biología del Desarrollo, Universidad Pablo de Olavide, Carretera de Utrera km 1, 41013 Seville, Spain

3 Current address: Max Plank Institute of Molecular Cell Biology and Genetics, Pfotenhauerstraße 108, 01307 Dresden, Germany

Author for correspondence: lazaro.centanin@cos.uni-heidelberg.de

Keywords: developmental timing, genetic chimera, inter-species transplantation, organogenesis, medaka, zebrafish, retina, lens induction, retina-tectal projection.

Abstract

The path from a fertilised egg to an embryo involves the coordinated formation of cell types, tissues and organs. Developmental modules (Raff, 1996) comprise discrete units specified by self-sufficient genetic programs that can interact among each other during embryogenesis. Here we took advantage of the different span of embryonic development between two far related teleosts, zebrafish (*Danio rerio*) and medaka (*Oryzias latipes*), of 3 and 9 days respectively, to explore modularity principles. We report that inter-species blastula transplantations result in the ectopic formation of a retina formed by donor cells — a module. We show that the developmental time of the retina follows a genetic program: an ectopic zebrafish retina in medaka develops with zebrafish dynamics. Heterologous transplantation results in a temporal decoupling between the donor retina and host organism, illustrated by two paradigms that require retina-host interactions: lens recruitment and retino-tectal projections. Our results uncover a new experimental system to address temporal decoupling along embryonic development, and highlight the presence of largely autonomous but yet interconnected developmental modules orchestrating organogenesis.

Introduction

In vertebrates, organogenesis takes place during embryonic development and follows a stereotypic, species-specific timing. Cases in which two organs of the same type are generated within an organism — eyes, ears, lungs, kidneys, gonads — indicate that these develop in a synchronized manner despite constituting independent units. The temporal control of organogenesis is of paramount importance to secure a functional coordination of organs within systems, i.e. neurons in a sensory organ should mature and become functional together with their target regions. A long-standing question in the field is whether neural organs follow an endogenous timing that defines the onset of neurogenesis — the autonomous timing —, or if alternatively, there are global signals that guarantee coordination among cell types, tissues, and organs — the ontogenic timing.

The vertebrate neural retina constitutes a major model for neurogenesis in the central nervous system (CNS), and it has been long ago demonstrated that the different types of retinal neurons are formed in a stereotypic temporal order, and arranged in dedicated layers (Livesey and Cepko, 2001). Retinal organoids and aggregates demonstrated that the vertebrate retina is capable of autonomously patterning (Eiraku et al., 2011), earlier suggested by the transplantation of optic vesicles into ectopic regions of the chick and fish (Gestri et al., 2018)(Picker et al., 2005). Although the self-organizing properties of the neural retina were demonstrated for other organoids, the inherently artificial conditions to develop 3D cultures, or the technical artifacts that accompany the transplantation of an optic cup, might affect the temporal sequence of biological processes on organoids or aggregates (DiStefano et al., 2018). The ideal set up to explore developmental timing, therefore, should exploit the self-organizing properties of the retina while developing in a homo – or heterochronic physiological environment.

Teleost fish represent the vertebrate clade with most species, which span across a huge range of sizes, body shapes and times of embryonic development (Betancur-R et al., 2017). Among teleost fish, *Danio rerio* and *Oryzias latipes* (zebrafish and medaka, respectively) have diverged some 250 million years ago, and belong to two of the most distant subgroups (Schartl et al., 2013). One of the most obvious differences between them is the time that they take to complete embryonic development, 3 days for zebrafish and 9 days for medaka (Figure 1). Here, we use zebrafish-medaka inter-species chimeras to report that isochronic transplantation of blastomeres from one species into the other results in the formation of an ectopic retina formed by donor cells. Our set up is unique since the entire developmental process from a blastomere to a differentiated retinal neuron (i.e. patterning, morphogenesis and neurogenesis) happens within the host species. Taking advantage that donor cells do not intermingle with host cells, we follow intrinsic and extrinsic properties of an

entire *module* on a physiological environment. We use fluorescent transgenic reporters, *in vivo* imaging and RNA-seq analysis to show that the ectopic cluster uses host cues to trigger a retinal transcriptional program. This program, however, follows the temporal logic of the donor species and forms heterochronic retinal neurons compared to the ones in the host retinae. Heterochronic neural development has phenotypic consequences that we illustrate using inter-lineage communication paradigms, as the induction of the lens by the retinal vesicle and the navigation of retinal axons to their target optic tectum. Altogether, we present an experimental set up to study developmental dynamics, use it to report a genetic timing in the execution of the retinal transcriptional program in vertebrates, and illustrate the consequences of heterochronic neurogenesis.

Results

Medaka / zebrafish inter-species transplantation results in the formation of ectopic retinae

Genetic chimeras formed by transplanting blastomeres from one fish embryo to another have been extensively used in zebrafish (Figure 1, left) and medaka (Figure 1, right), i.e to define the cell-autonomous vs cell-non-autonomous roles of novel mutant lines, to study lineages during embryonic and post embryonic development, *etc.* (Centanin et al., 2011; Haas and Gilmour, 2006; Poggi et al., 2005; Vogeli et al., 2006; Winkler et al., 2000). Intra-species transplantations at blastula stage results in donor and host cells mixed along the developing embryo. This was indeed the case when we transplanted blastomeres from ubiquitously labelled transgenic lines (*ßactin*::CAAX-EYFP in zebrafish, *Wimbledon* or *Gaudi*$^{LoxP.OUT}$ in medaka)(Centanin et al., 2014; Centanin et al., 2011) into non-labelled controls from the same species (Figure 2A, B)(N>20 transplantation experiments for each species, N>10 embryos per transplantation experiment). We have observed that in trans-species transplantations, however, donor cells stay clustered together and do not mix with host cells during gastrulation, both for zebrafish-to-medaka (zebraka, Figure 2C) and for medaka-to-zebrafish (medrafish, Figure 2D)(N = 17 transplantation experiments, N > 100 chimeras for zebraka; N = 33 transplantation experiments, N > 100 chimeras for medrafish; a *transplantation event* is a transplantation experiment performed on a given day with a specific donor-host combination, that lead to one or more chimeras of the described phenotype)(Supplementary Table 1, 2). In both zebraka and medrafish, host blastomeres can proceed through gastrulation and a body axis is evident at 19 hours post-transplantation (hpt) (Figure 2C, D). Stunningly, the cluster of transplanted cells often develops into an ectopic organ that resembled a retina, which is formed by EGFP-positive cells (Figure 3A, B). We have observed ectopic retinae for both trans-species transplantation setups, frequently containing retinal pigmented epithelium (Figure 3B, see also Figure 5C''), which indicates

that the initial alien cluster followed a developmental program despite of not intermingling with host cells during epiboly.

The formation of an ectopic retina in medaka-zebrafish chimera is highly reproducible, having observed the same phenotype consistently on different transplantation experiments using diverse transgenic donors and hosts (16 out of 21 transplantation experiments for zebraka, 29 out of 37 transplantation experiments for medrafish; on a representative experiment using heterozygote transgenic founders, we obtained 23 zebrakas out of 72 transplanted embryos) (Supplementary Table 1, 2). The expression of retinal transcripts in the cluster was confirmed by using transcriptional reporters for retinal progenitors and retinal neurons in medaka, namely *Rx2 - retinal homeobox factor 2* (Inoue and Wittbrodt, 2011; Reinhardt et al., 2015; Winkler et al., 2000) and a*toh7* (Del Bene et al., 2007; Kay et al., 2005; Poggi et al., 2005; Souren et al., 2009). When blastomeres from medaka Tg(*Rx2*:H2B-RFP) were transplanted into non-labelled zebrafish blastulae, the retinal-like cluster expressed the medaka retinal reporter *Rx2* (Figure 3C) (Supplementary Table 2). The same result has been obtained when we used Tg(*Atoh7*:EGFP) as donors, suggesting that the ectopic cluster has both retinal identity and the potential to trigger neurogenesis (Figure 3D) (Supplementary Table 2).

Molecular confirmation and morphological characterisation of ectopic retinae.

There are a number of methods available to address species-specific contribution of transcripts in a chimera (Ealba and Schneider, 2013). The low sequence identity of homologous genes between zebrafish and medaka allows segregating the bulk transcriptome of chimerae *in silico*, therefore expanding the analysis of the transcriptional profile in ectopic retinae of zebrakas. We compared RNA-seq from zebrafish, medaka, and zebraka embryos at 48 hpf, a stage in which neurogenesis has started in zebrafish but it is only about to start in medaka. We selected chimeras with a clear EGFP+ cluster close to one of the endogenous retinae, as these are the most likely to become a retina. As expected, the transcriptome from zebrafish, but not the one from medaka, aligned to the zebrafish genome (Figure 3E, Supplementary Figure 1). Due to the large evolutionary distance, only a few RNA-seq reads form the medaka transcriptome mapped on the zebrafish genome (Supplementary Figure 1), and these displayed a distinguishable morphology as well as a minimal number of reads (Supplementary Figure 1). In contrast, numerous reads from the transcriptome of zebrakas, consisting in a full medaka transcriptome plus a partial transcriptome from the few zebrafish cells, could be aligned to the zebrafish genome (Figure 3E, Supplementary Figure 1, Supplementary Table 3). These peaks corresponded to genes that are expressed by the zebrafish retina at the same developmental time (*vsx2, rx1, rx2* among others, Figure 3E, Supplementary Table 4 and Supplementary Figure 2). Genes exclusively expressed in other organs at the same

stage, and therefore present in the zebrafish transcriptome (i.e., cardiac muscle) were absent in the zebraka transcriptome (Figure 3E and Supplementary Table 4). This analysis confirms the molecular retinal identity of the EGFP+ cluster in zebrakas chimeras.

The vertebrate retina displays a stereotypic distribution of cell types arranged in defined nuclear layers (Centanin and Wittbrodt, 2014), most evident when analysed in cryo-sections (Figure 4A-A'''). To address the layering and cellular organization of the ectopic retina in both zebraka and medrafish, we grew chimeras until late embryc stages – 9 dpf. for zebraka, 5 dpf. for medrafish. Retinae were analysed by DAPI nuclear staining either in whole-mounts and/or in cryo-sections.

A whole-mount analysis of 9 dpf zebraka revealed that the ectopic retina was not organised in the three classical nuclear layers, but lamination could still be observed on patches within the ectopic cluster (Figure 4B-C'', white arrows). The examination of ectopic clusters in chimeras where Tg(*atoh7*:EGFP) were used as donors allowed following the occurrence of RGCs and their axons. Notably, EGFP+ cells usually localized adjacent to each other, as it is the case in the endogenous retina, forming pseudo layers in the ectopic retinae (Figure 4B''', C-C''). The internal organization of cell types is more apparent when analyzing cryo-sections of zebraka and medrafish ectopic retinae by DAPI, membrane label and/or cell type specific antibodies (Figure 5). A zebraka ectopic retina (Figure 5A, B top) from Tg(*ßactin*:CAAX-EGFP) donors typically displays a row of nuclei (Figure 5A', B') separated from other cells in the organ by a space filled in by membranes (Figure 5A'', B'), resembling an outer plexiform layer (compare to Figure 4A). Staining with an anti-Rx2 antibody (Inoue and Wittbrodt, 2011) that recognizes retinal progenitors and photoreceptors (Figure 4A'-A'''), indicates that these cells indeed express photoreceptor molecular markers. The same distribution of nuclei (Figure 5C, C', C'', D) and signal using a Rx2 antibody (Figure 5 D'') can be seen in the ectopic retinae of medrafish, which also display an RPE cell layer that gets indeed pigmented (Figure 5C''). Further attempts to detect additional cell types in the neural retina, using specific antibodies against cells present in the INL, did not result in any significant staining (Figure 5D' and data not shown). Overall, our experiments reveal that both in zebraka and medrafish, the ectopic retinae include patches of lamination and clusters of differentiatied RGCs and photoreceptors.

It has long been proposed that neural ectoderm constitutes the default differentiation program for early embryonic cells. Indeed, neural retina was the first *organoid* produced in 3D cultures from an aggregate of embryonic stem cells (ESCs)(Eiraku et al., 2011), followed by other neural organs (Lancaster et al., 2013; Suga et al., 2011). In zebraka and medrafish chimeras, we have noticed that ectopic retinae inevitably form adjacent to an endogenous retina (Figure 3A, B, N>60 chimerae). We have never observed an ectopic retina in remote locations, which strongly suggests that positional information from the host can be decoded by the transplanted cells - although does not elucidate whether the host anlage has a permissive or an inductive role. Retinal identity is not

the only fate that ectopic blastocysts can adopt when transplanted into the foreign species, since we have observed clusters differentiating into vasculature or pigmented cells (Supplementary Figure 3) (Hong et al., 2012). The ectopic retina obtained in the present inter-species transplantation protocol, however, is the only organ entirely composed of foreign cells (Figure 3A, 5A'', 5C', 5D') and as such, permits a compartmentalised analysis of host and donor organs going through embryonic development in parallel and in the same embryonic environment.

Ectopic retinae differentiation follows a genetic timing

The onset of retinal neurogenesis in medaka and zebrafish occurs at different hours post-fertilization (hpf). We decided to use the inter-species chimeras as a paradigm to address developmental timing, i.e., to explore whether retinal neurogenesis follows an intrinsic temporal program (*genetic* timing) or if alternatively, it responds to signals from neighbour tissues operating as temporal coordinators (*ontogenic* timing). Using the transcriptome data that we obtained from zebrakas at 48 hpf, we aimed at analysing the relative expression of progenitor and neurogenic genes in the ectopic retinae. We used *rx3* and *vsx2* as retinal progenitor markers and *atoh7*, *ptf1a* and *pou42* as neurogenic/differentiation markers (Barabino et al., 1997; Jusuf and Harris, 2009; Kay et al., 2001; Loosli et al., 2003), and compared their expression ratios in zebrafish, medaka and zebrakas, using as a scaffold published transcriptomes from zebrafish and medaka at different developmental stages (Marlétaz et al., 2018). We noticed that ratios in the medaka transcriptome of zebraka match those of wild type medakas, while ratios in the zebrafish transcriptome of zebrakas are consistently found closer to the zebrafish control (Supplementary Figure 4). We have extended this approach to include all retinal genes, by performing PCA analysis using zebrafish and medaka orthologs that are expressed in the retina and using ratios to *rx3* and *vsx2* as internal reference (Figure 6 A, B). Again, we observed that the medaka transcriptome from zebrakas (zebraka:medaka) groups with medaka controls. The zebrafish component of zebraka (zebraka:zebrafish), however, occupies a very different position falling closer to the zebrafish control. These results indicate that despite developing in a foreign species, a zebrafish retina in zebraka does not follow the differentiation pace occurring in the host but rather maintains its own differentiation dynamics resulting in a premature generation of retinal neurons.

To confirm the genetic timing of retinogenesis in zebrakas *in vivo*, we performed transplantations using a Tg(*atoh7*:EGFP) zebrafish as a donor. Retinal ganglion cells (RGCs) represent the first cell type to differentiate in the vertebrate neural retina, and *atoh7* has extensively been used as a marker to follow the onset of RGCs in both zebrafish and medaka (Del Bene et al., 2007; Kay et al., 2005; Poggi et al., 2005; Souren et al., 2009). Fluorescent proteins under the control of an *atoh7* promoter can be detected at 26 hpf in zebrafish and one day later (50hpf) in medaka, in progenitor cells that

are poised to generate RGCs (Poggi et al., 2005; Souren et al., 2009). We transplanted transgenic Tg(*atoh7*:EGFP)(*ef1*:LynTomato) zebrafish blastocysts into unlabelled medaka blastula and observed the onset of EGFP expression by 26 hpf, ca. 24 h before the expression of the endogenous medaka *atoh7* (N = 3)(Figure 6C-C''). This result confirms and complements our transcriptome analysis and indicate once again that the trigger for RGC generation follows a genetic timing irrespective of the timing of their neighbouring organs.

Extensive arborisation from zebrafish RGCs in the medaka optic tectum.

The generation of premature RGCs by the ectopic EGFP+ cluster has consequences in the host that we revealed by analysing axon innervation of RGCs in zebrakas and medrafish. In vertebrates, RGCs projections group in an optic nerve that migrate from the retinae to their target region in the brain, the visual cortex in mammals and the optic tectum in fish. In zebrafish and medaka, each retina project an optic nerve to the contralateral optic tectum (Baier et al., 1996; Yoda et al., 2004). We noticed that in zebrakas where donor cells were either Tg(*atoh7*:EGFP) or Tg(*ßactin*::CAAX-EYFP), zebrafish RGCs generate axons that travelled to the medaka optic tectum despite the ectopic position of the retina (Figure 6D, E). The RGCs axons from one ectopic retina usually innervated both *ipsi* and *contralateral* optic tecta (Figure 6E). The premature birth of zebrafish RGCs guarantees that their projections arrive to the target tissue earlier than the endogenous optic nerve, which results in a substantial innervation of the medaka tecta by the zebrafish RGC projections (Figure 6E). Following the same rationale, the medaka RGC projections in medrafish arrive to the zebrafish tecta later that the endogenous nerve, and therefore their ramification is reduced (Supplementary Figure 5). These observations reveal a hetero-chronic formation of the same cell type within a chimeric embryo, following a genetic timing of differentiation despite sharing the physiological domain.

We observed examples in which the earlier formation of zebrafish RGCs resulted in anomalous axon projections in zebrakas, evidencing that RGC projections can indeed highjack on ectopic paths that are present at the time of navigation. That was the case for seven zebrakas - using either Tg(*ßactin*::CAAX-EYFP) or Tg(*atoh7*:EGFP) as donor, N=5 and N=2 respectively -, in which the RGCs projected along the lateral line nerve (Figure 6F), which is present in the embryo before the pathfinding cues to reach the optic tecta. These miss-projections usually reached the caudal fin, evidencing a promiscuous behaviour of the zebrafish RGC axons in medaka hosts. Since these chimeras all projected to the optic tecta as well (Figure 6F), our interpretation is that the earlier development of the lateral line nerve might have offered a permissive migratory route. Our results indicate that even when medaka and zebrafish blastocysts do not intermingle during epiboly and axis formation, differentiated cells can later on recognise cues present in the host, as those necessary for axonal pathfinding.

Different sources for lens recruitment in zebraka and medrafish.

The vertebrate eye is composed of the neuroepithelial derivatives, i.e. the neural retina (NR) and the retinal pigmented epithelium (RPE), which differentiate from a common progenitor pool (Holt et al., 1988; Poggi et al., 2005) (Wetts and Fraser, 1988), and additional tissues in the anterior segment of the eye that derive from different germ layers (Soules and Link, 2005). The lens, a distinctive feature of the vertebrate eye, derives from the surface ectoderm and its formation is induced by retinal progenitors during early retinogenesis (Soules and Link, 2005). Lens induction therefore constituted yet another paradigm to assess inter-relations between donor and host tissues in chimeric embryos. When analysing the transcriptomes of zebrakas, we noticed that although retinal genes were represented (Figure 3E), lens transcripts from the donor were absent in the chimeras (Figure 7A). This indicate that the lens that is evident in zebraka either expresses a different set of transcripts or alternatively, it was formed using cells from the host.

We performed blastula transplantations using EGFP+ blastomeres from zebrafish into the *cryA*:eCFP line from medaka, which labels the endogenous lenses with a cyan fluorescent protein (Centanin et al., 2014). When generated using this set up, zebrakas display an ectopic zebrafish retina which lens expresses the medaka *cry*:EGFP transgene (Figure 7B-B"). This clearly indicates that zebrafish retinal cells recruited medaka host cells to form an ectopic lens. In the context of our previous observations showing that in zebrakas the ectopic retina develops earlier than the host retinae, our results evidence that the surface ectoderm has the potential to become a lens before the stage at which it is recruited endogenously in medaka. Surprisingly, this situation differs in the case of medrafish. When we transplant blastomeres from a medaka *cryA*:ECFP, *Gaudi*^{LoxPOUT} into unlabelled zebrafish host, we noticed that the ectopic retina displays a cyan lens (Figure 7C-C", see also Figure 5C')(N=10 transplantation events). These results reveal that, in contrast to the case in zebrakas, the ectopic medaka neural retina does not induce lens formation from zebrafish surface ectoderm. Therefore, the EGFP+ medaka cluster in medrafish generates both the retina and anterior structures of the eye like the lens. It is therefore valid to speculate that by the time the medaka retina starts the lens induction program, the surface ectoderm in zebrafish is no longer competent to acquire lens identity. Temporal windows for inductive process have been reported in other systems like the Hensen's node in chicken, and the Spemann-Mangold organiser in frogs (Anderson and Stern, 2016; Hensen, 1876; Inagaki and Schoenwolf, 1993; Mangold and Spemann, 1927; Martinez Arias and Steventon, 2018; Spemann and Mangold, 2001; Storey et al., 1992; WADDINGTON, 1934).

Discussion

Trans-species transplantations have been long used in developmental biology to address the most diverse subjects. Examples of such an approach can be found almost a century ago, when Harrison, Twitty and colleagues transplanted eye cups and limbs between two salamander species of different sizes – the large *Ambysioma tigrinum* and the smaller *Ambysioma punctatum* (Harrison, 1929; Twitty and Schwind, 1928; Twitty and Schwind, 1931). Their experiments revealed an intrinsic (*genetic*) control for organ size and evidence for an organ intrinsic growth rate, since the transplanted *rudiment* (either eyes or limbs) reached the size of the donor species. An *A.tigrinum* eye transplanted into *A.punctatum* outgrows the endogenous eyes at the same rate as the undisturbed control organ in the donor species, while an *A.punctatum* eye transplanted into *A.tigrinum* will remain smaller than its endogenous counterparts (Twitty and Schwind, 1931). During the 70's, Nicole Le Dourain pioneered the now classical quail-to-chick transplantation as a method to follow the lineage of neural crest cells, using distinct nuclear properties between both species that were obvious under a regular microscope (Le Douarin, 1973; Le Douarin, 2004; Le Douarin and Teillet, 1973). Other examples where pieces of tissues were transplanted from one species to another include graft transplantations from *Planaria dorotocephala* to *Planaria maculata* to demonstrate the potency of regenerating cells (Santos, 1929; Santos, 1931), and grafting different plant species to address horizontal genome transfer and speciation (Fuentes et al., 2014).

Inter-species chimeras have also been generated at earlier developmental stages by mixing blastomeres. In fish, this approach has led to the characterization of primordial germ cell (PGC) migration to their respective gonad (Saito et al., 2010), providing a valuable resource for expanding endangered species. Work using mammals include the early rat-to-mice blastomere transplantation (Gardner and Johnson, 1973), used later on to address the 'empty niche' hypothesis (Kobayashi et al., 2010). Briefly, the authors used mutant hosts unable to generate a defined organ and showed that the transplanted, donor blastomeres were able to colonise the *empty niche* and form the missing organ – i.e, a viable mouse with a rat pancreas (Kobayashi et al., 2010). Interestingly, and in contrast with the experiments from Harrison and Twitty mentioned earlier, the donor organ adjusts to the size of the host species – a rat pancreas within a mouse has the size of a mouse pancreas -, revealing different strategies for organ control in different species, whether these differences are organ or species specific remains an interesting question. Inter-species chimerae were also generated using human cells, most famously via heterochronic transplantation into mice to assess teratoma formation, but also combining blastomeres with those of other species. Human-to-pig chimera, for instance, were used to explore developmental boundaries of pluripotent stem cell transplantations in different mammals (Wu et al., 2016; Wu et al., 2017). Besides the vast literature on inter-species transplantations, the topic of developmental timing was barely approached. A recent example

involves transplanting ESC-derived cortical cells to assess the dynamics of neuronal differentiation, using human cortical neurons (where maturation takes months to years) transplanted into mice (where maturation takes a few weeks) (Linaro et al., 2019). The authors report that transplanted human neurons go through an extended maturation period compared to their mice counterpart, retaining juvenile properties even when the host mice was already an adult.

Here, we developed a new experimental set-up complimentary to the previously mentioned, where the entire developmental history of an organ unfolds in an alien species - from a blastomere to a retinal neuron. Notably, the entire process happens using host and donor species that are not genetically modified to facilitate or induce grafting. We combined blastomeres of species that diverged 250 My ago and observed that although initially, cells grouped — or stayed grouped — in a species-specific fashion, later on the exogenous cluster interacts with the biochemical and/or physical environment of the host. Albeit not participating into the host morphogenesis, the cluster expresses different retinal maker genes and generates retinal cell types. We exploit the fortuitous formation of a retina to explore intrinsic and extrinsic temporal properties of retinogenesis, i.e. the generation of defined cell types (tissue specific) and the interaction with the host for inductive and navigation processes (non-tissue specific, lens formation and optic nerve pathfinding, respectively). We found that the cluster can originally read signals from the host to trigger the retinogenesis program, since ectopic retinae are always found adjacent to one endogenous eye. Yet despite this interaction with the host, ectopic retinae followed a species-specific developmental time. On the molecular side, we combine fluorescent reporters, *in vivo* imaging and RNA-seq analysis to show that trans-species retinae are formed by reproducing the dynamics of the well-described transcriptional cascades responsible for retinogenesis in the host species. Finally, the heterochronic retina can still interact with different host tissues to induce the formation of a lens using the host surface ectoderm (in zebrakas) and read molecular cues from the host to navigate axonal outgrowth to the proper, endogenous targets. Therefore, our experiments add to the growing evidence on autonomous organisation of biological systems (Eiraku et al., 2011; Sato et al., 2009; van den Brink et al., 2014) with a focus on developmental dynamics and demonstrate an evolutionary conserved compatibility between the ectopic retina and the host environment.

It has recently been suggested that in mammals, developmental timing depends on differential biochemical reactions (Matsuda et al., 2020), specifically on protein stability (Rayon et al., 2020), a kinetic parameter that has species-specific features. Whether the same holds true for an entire extrinsic organ developing in a different host species is an attractive hypothesis that needs to be formally tested. Regardless of the molecular nature of the intrinsic timing, our results illustrate the temporal window in which a tissue can be induced into another (i.e., surface ectoderm into a lens), which proved to be way broader than the temporal requirements during embryonic development.

Overall, our experiments report a successful chimerism between vertebrate species that differ more than 250 My ago, the highest distance for an isochronic transplantation in such an early embryonic stage. Using this novel inter-species paradigm to tackle temporal aspects of embryonic development, we could reveal some basic principles predicted by the modularity hypothesis (Raff, 1996). Thus, here we show that the evolutionary conserved "retinal module" can be defined both by its intrinsic genetic identity and its external connectivity to neighboring modules.

Materials and Methods

Fish stocks and transgenic fish lines

Medaka (*Oryzias latipes*) and Zebrafish (*Danio rerio*) stocks were maintained according to the local animal welfare standards (Tierschutzgesetz §11, Abs. 1, Nr. 1). Animal experiments were performed in accordance with European Union animal welfare guidelines (Tierschutzgesetz 111, Abs. 1, Nr. 1, Haltungserlaubnis AZ35–9185.64 and AZ35–9185.64/BH KIT).

The following zebrafish lines were used in this study: AB zebrafish strain as a wildtype, *OlBactin2:*EGFP-CAAX (Centanin et al., 2011), *Atoh7*:GFP (Del Bene et al., 2007), *ef1a*:Lyn-Cherry

The following medaka lines were used in this study: Cab strain as a wild type, Heino (Albino medaka), Wimbledon DsTrap#6 (Centanin et al., 2011), *Rx2*::H2B-mRFP (Inoue and Wittbrodt, 2011), *zFli1*::EGFP (Schaafhausen et al., 2013), Gaudi^{RSG} (contains the integration reporter crya:ECFP that drives ECFP expression in the lens), Gaudi^{LoxPOUT} (Centanin et al., 2014), *Atoh7*::EGFP (Del Bene et al., 2007), *Atoh7*::lynTdTomato (Lust et al., 2016).

Intra- and Inter-species transplantation

Zebrafish crosses were set up at 10 a.m, collected after 20 min and kept at room temperature. Medaka couples were maintained together and produced from 8:00 am on. Medaka eggs were collected between 9.00 and 10.30 a.m. and grown at 32°C to synchronize embryos at blastula stage. Blastula stage embryos were dechorionated as previously described using hatching enzyme for medaka and pronase (30mg/ml) for zebrafish, and placed for transplantation in agarose wells with the proper medium for the host species (E3 medium for zebrafish or ERM for medaka).

One blastula could be used as a donor for 3-5 hosts, 20 to 50 cells were transplanted from the animal pole region of the donor to the hosts animal pole. Transplantations were carried out as previously described (Rembold et al., 2006). Transplanted embryos were kept in growth medium of the host species. In accordance with animal welfare standards transplantations with Zebrafish hosts were maintained up to day 5 of embryonic development and Medaka hosts were grown to day 9 of embryonic development.

Antibodies and staining

Primary antibodies used in this study were rabbit anti-GFP (Live technologies, 1/750), chicken anti-GFP (Invitrogen, 1/750), rabbit α-DsRed (1/500), rabbit anti-Rx2 (1/200)(Reinhardt et al., 2015), mouse anti-GS (Millipore, 1/100), rabbit anti-Prox1 (Millipore, 1/100). Secondary antibodies were Alexa488 anti-rabbit, Alexa488 anti-chicken, Alexa546 anti-mouse, Alexa 647 anti-rabbit (Live Technologies 1/500) and Dylight 548 anti-rabbit, Dylight 647 anti-mouse (Jackson 1/500). DAPI was used in a final concentration of 5 ug/l. Cryo-sections were done as previously described (Reinhardt et al., 2015).

Imaging

Stained embryos were imaged with a laser-scanning confocal microscope Leica TCS SP8 (20x immersion objective) or a Leica TCS SPE. Imaging was done on glass-bottomed dishes (MatTek Corporation, Ashland, MA 01721, USA).

Live embryos were anaesthetized in 1mg/ml Tricaine in the respective fish medium as described by Seleit et al. 2017 (Seleit et al., 2017) and imaged in 3% Methylcellulose in ERM or in 0.6% low melting agarose in ERM. Embryos were screened and imaged using a Stereomicroscope (Olympus MVX10 MacroView) coupled to a Leica DFC500 camera or at a laser-scanning confocal microscope Leica TCS SP8 (20x immersion objective) or Leica TCS SPE. All subsequent image analysis was performed using Fiji software (Schindelin et al., 2012).

RNA seq on Zebrakas.

Zebrakas with an EGFP+ cluster in the head were used to extract total RNA (**Trizol**) at 50hfp, together with zebrafish (donor) and medaka (host) embryos that were grown at the same temperature (experiments done in triplicates). Libraries were prepared from total RNA followed by a polyA selection (NEBnext PolyA) and sequenced in a NextSeq 500 platform in 85-nt single end reads. The number of duplicates for both zebrafish and medaka samples is two, whereas zebraka experiment was performed in triplicate. Datasets can be accessed at GEO: GSE150009. RNA-seq samples were mapped against both oryLat2 and danRer10 assemblies using Hisat2 (Kim et al., 2015). A summary on the number and percentage of mapped reads on both genomes can be found in Table X. The aligned SAM files were assembled into transcripts and their abundance was estimated Cufflinks v2.2.1 (Trapnell et al., 2012). The DEG analysis between the Zebrafish and Zebraka transcriptome was also performed with Cufflinks v2.2.1. For downstream analyses, only the Zebraka upregulated genes have been considered, in order to avoid a library size bias given by the difference in number of mapped reads in the two datasets (complete list in Supplementary Dataset 1). GO enrichment was calculated with the tool FishEnrichr (Kuleshov et al., 2016). PCA analysis was performed using a subset of genes selected according the following criteria: (i) genes expressed

in the eye between 24h and 48h in zebrafish retrieve from ZFIN database (Ruzicka et al., 2019); (ii) with an expression value > 10 FPKM in Zebraka and (iii) sharing a direct orthologue in medaka. The final list of gene fulfilling all three criteria comprised 817 genes (complete list in Supplementary Dataset 2). The inter-species expression differences were normalized for the expression value of the progenitor markers rx3 (rax) and vsx2. Zebraka FPKM ratios between retinal developmental progression genes (*atoh7, ptf1a and pou4f2*) and retinal progenitor markers (*rx3 and vsx2*) were compared with the same ratios from wt medaka and zebrafish transcriptomes at resembling developmental stages (Marlétaz et al., 2019) In the case where both the numerator and the denominator of the ratio were equal to zero, the resulting value was also reported as zero.

Acknowledgments

We are tankful to the Centanin and S. Lemke groups, J. Wittbrodt and A. Martinez Arias for scientific input on earlier version of the manuscript, J. Wittbrodt for access to confocal microscopes and fish stocks, J. Lohmann and T. Greb for feedback on plant inter-species transplantation experiments, N. Foulkes for constructive input regarding developmental dynamics, S. Frings and his group for allowing access to the cryostat, E. Leist, M. Majewski and A. Saraceno for fish husbandry. This work was supported by grants from the Deutsches Forschungsgemeinshaft to L.C. (SFB873 – A11) and the Spanish Ministry of Science, Innovation and Universities (MICINN) to J-R.M.M.: BFU2017-86339P and MDM-2016-0687. LB contract is supported by Fundación Ramón Areces-2016.

Author Contributions

Conceptualization, LC; Methodology, JFF, LC; Software, LB, JRMM; Validation, JF; Formal Analysis, JFF, LB, LA, JRMM, LC; Resources, JRMM, LC; Writing – Original Draft Preparation, LC; Writing – Review & Editing Preparation, JFF, JRMM, LC; Visualization, JFF, LB; Supervision, LC; Project Administration , LC; Funding Acquisition, JRMM, LC.

Declaration of Interests

The authors declare no competing interests.

References

Anderson, C. and Stern, C. D. (2016). Organizers in Development. *Curr Top Dev Biol* **117**, 435-454.

Baier, H., Klostermann, S., Trowe, T., Karlstrom, R. O., Nusslein-Volhard, C. and Bonhoeffer, F. (1996). Genetic dissection of the retinotectal projection. *Development (Cambridge, England)* **123**, 415-425.

Barabino, S. M., Spada, F., Cotelli, F. and Boncinelli, E. (1997). Inactivation of the zebrafish homologue of Chx10 by antisense oligonucleotides causes eye malformations similar to the ocular retardation phenotype. *Mech Dev* **63**, 133-143.

Betancur-R, R., Wiley, E. O., Arratia, G., Acero, A., Bailly, N., Miya, M., Lecointre, G. and Ortí, G. (2017). Phylogenetic classification of bony fishes. *BMC Evolutionary Biology* **17**, 162.

Centanin, L., Ander, J.-J., Hoeckendorf, B., Lust, K., Kellner, T., Kraemer, I., Urbany, C., Hasel, E., Harris, W. A., Simons, B. D., et al. (2014). Exclusive multipotency and preferential asymmetric divisions in post-embryonic neural stem cells of the fish retina. *Development (Cambridge, England)* **141**, 3472-3482.

Centanin, L., Hoeckendorf, B. and Wittbrodt, J. (2011). Fate restriction and multipotency in retinal stem cells. *Cell Stem Cell* **9**, 553-562.

Centanin, L. and Wittbrodt, J. (2014). Retinal neurogenesis. *Development (Cambridge, England)* **141**, 241-244.

Del Bene, F., Ettwiller, L., Skowronska-Krawczyk, D., Baier, H., Matter, J.-M., Birney, E. and Wittbrodt, J. (2007). In vivo validation of a computationally predicted conserved Ath5 target gene set. *PLoS genetics* **3**, 1661-1671.

DiStefano, T., Chen, H. Y., Panebianco, C., Kaya, K. D., Brooks, M. J., Gieser, L., Morgan, N. Y., Pohida, T. and Swaroop, A. (2018). Accelerated and Improved Differentiation of Retinal Organoids from Pluripotent Stem Cells in Rotating-Wall Vessel Bioreactors. *Stem cell reports* **10**, 300-313.

Ealba, E. L. and Schneider, R. A. (2013). A simple PCR-based strategy for estimating species-specific contributions in chimeras and xenografts. *Development* **140**, 3062-3068.

Eiraku, M., Takata, N., Ishibashi, H., Kawada, M., Sakakura, E., Okuda, S., Sekiguchi, K., Adachi, T. and Sasai, Y. (2011). Self-organizing optic-cup morphogenesis in three-dimensional culture. *Nature* **472**, 51-56.

Fuentes, I., Stegemann, S., Golczyk, H., Karcher, D. and Bock, R. (2014). Horizontal genome transfer as an asexual path to the formation of new species. *Nature* **511**, 232-235.

Gardner, R. L. and Johnson, M. H. (1973). Investigation of early mammalian development using interspecific chimaeras between rat and mouse. *Nat New Biol* **246**, 86-89.

Gestri, G., Bazin-Lopez, N., Scholes, C. and Wilson, S. W. (2018). Cell Behaviors during Closure of the Choroid Fissure in the Developing Eye. *Front Cell Neurosci* **12**, 42.

Haas, P. and Gilmour, D. (2006). Chemokine signaling mediates self-organizing tissue migration in the zebrafish lateral line. *Developmental cell* **10**, 673-680.

Harrison, R. G. (1929). Correlation in the development and growth of the eye studied by means of heteroplastic transplantation. *Wilhelm Roux' Archiv für Entwicklungsmechanik der Organismen* **120**, 1-55.

Hensen, V. (1876). Beobachtungen über die Befruchtung und Entwicklung des Kaninchens und Meerschweinchens. *Z. Anat. Entw. Gesch* **1:**, 353-423.

Holt, C. E., Bertsch, T. W., Ellis, H. M. and Harris, W. A. (1988). Cellular determination in the Xenopus retina is independent of lineage and birth date. *Neuron* **1**, 15-26.

Hong, N., Chen, S., Ge, R., Song, J., Yi, M. and Hong, Y. (2012). Interordinal chimera formation between medaka and zebrafish for analyzing stem cell differentiation. *Stem cells and development* **21**, 2333-2341.

Inagaki, T. and Schoenwolf, G. C. (1993). Axis development in avian embryos: the ability of Hensen's node to self-differentiate, as analyzed with heterochronic grafting experiments. *Anatomy and Embryology* **188**, 1-11.

Inoue, D. and Wittbrodt, J. (2011). One for all--a highly efficient and versatile method for fluorescent immunostaining in fish embryos. **6**, e19713.

Jusuf, P. R. and Harris, W. A. (2009). Ptf1a is expressed transiently in all types of amacrine cells in the embryonic zebrafish retina. *Neural Dev* **4**, 34.
Kay, J. N., Finger-Baier, K. C., Roeser, T., Staub, W. and Baier, H. (2001). Retinal ganglion cell genesis requires lakritz, a Zebrafish atonal Homolog. *Neuron* **30**, 725-736.
Kay, J. N., Link, B. A. and Baier, H. (2005). Staggered cell-intrinsic timing of ath5 expression underlies the wave of ganglion cell neurogenesis in the zebrafish retina. *Development (Cambridge, England)* **132**, 2573-2585.
Kim, D., Langmead, B. and Salzberg, S. L. (2015). HISAT: a fast spliced aligner with low memory requirements. *Nature Methods* **12**, 357-360.
Kobayashi, T., Yamaguchi, T., Hamanaka, S., Kato-Itoh, M., Yamazaki, Y., Ibata, M., Sato, H., Lee, Y.-S., Usui, J.-I., Knisely, A. S., et al. (2010). Generation of rat pancreas in mouse by interspecific blastocyst injection of pluripotent stem cells. *Cell* **142**, 787-799.
Kuleshov, M. V., Jones, M. R., Rouillard, A. D., Fernandez, N. F., Duan, Q., Wang, Z., Koplev, S., Jenkins, S. L., Jagodnik, K. M., Lachmann, A., et al. (2016). Enrichr: a comprehensive gene set enrichment analysis web server 2016 update. *Nucleic Acids Res* **44**, W90-97.
Lancaster, M. A., Renner, M., Martin, C.-A., Wenzel, D., Bicknell, L. S., Hurles, M. E., Homfray, T., Penninger, J. M., Jackson, A. P. and Knoblich, J. A. (2013). Cerebral organoids model human brain development and microcephaly. *Nature* **501**, 373-379.
Le Douarin, N. (1973). A biological cell labeling technique and its use in expermental embryology. *Dev Biol* **30**, 217-222.
Le Douarin, N. M. (2004). The avian embryo as a model to study the development of the neural crest: a long and still ongoing story. *Mech Dev* **121**, 1089-1102.
Le Douarin, N. M. and Teillet, M. A. (1973). The migration of neural crest cells to the wall of the digestive tract in avian embryo. *J Embryol Exp Morphol* **30**, 31-48.
Linaro, D., Vermaercke, B., Iwata, R., Ramaswamy, A., Libe-Philippot, B., Boubakar, L., Davis, B. A., Wierda, K., Davie, K., Poovathingal, S., et al. (2019). Xenotransplanted Human Cortical Neurons Reveal Species-Specific Development and Functional Integration into Mouse Visual Circuits. *Neuron* **104**, 972-986 e976.
Livesey, F. J. and Cepko, C. L. (2001). Vertebrate neural cell-fate determination: lessons from the retina. *Nature reviews. Neuroscience* **2**, 109-118.
Loosli, F., Staub, W., Finger-Baier, K. C., Ober, E. A., Verkade, H., Wittbrodt, J. and Baier, H. (2003). Loss of eyes in zebrafish caused by mutation of chokh/rx3. **4**, 894-899.
Lust, K., Sinn, R., Pérez Saturnino, A., Centanin, L. and Wittbrodt, J. (2016). De novo neurogenesis by targeted expression of atoh7 to Müller glia cells. *Development (Cambridge, England)* **143**, 1874-1883.
Mangold, O. and Spemann, H. (1927). ÜBER INDUKTION VON MEDULLARPLATTE DURCH MEDULLARPLATTE IM JÜNGEREN KEIM, EIN BEISPIEL HOMÖOGENETISCHER ODER ASSIMILATORISCHER INDUKTION. *Wilhelm Roux Arch Entwickl Mech Org* **111**, 341-422.
Marlétaz, F., Firbas, P. N., Maeso, I., Tena, J. J., Bogdanovic, O., Perry, M., Wyatt, C. D. R., de la Calle-Mustienes, E., Bertrand, S., Burguera, D., et al. (2018). Amphioxus functional genomics and the origins of vertebrate gene regulation. *Nature* **564**, 64-70.
Martinez Arias, A. and Steventon, B. (2018). On the nature and function of organizers. *Development* **145**.
Matsuda, M. Hayashi, H., Garcia-Ojalvo, J., Yoshioka-Kobayashi, K., Kageyama, R., Yamanaka, Y., Ikeya, M., Toguchida, J., Alev, C., and Ebisuya, M. (2020). Species-specific segmentation clock periods are due to differential biochemical reaction speeds. *Science* **369**(6510): 1450-1455.
Picker, A. and M. Brand (2005). Fgf signals from a novel signaling center determine axial patterning of the prospective neural retina. *Development* **132** 4951-4962.
Poggi, L., Vitorino, M., Masai, I. and Harris, W. A. (2005). Influences on neural lineage and mode of division in the zebrafish retina in vivo. *The Journal of cell biology* **171**, 991-999.
Raff, R. A. (1996). *The Shape of Life: Genes, Development, and the Evolution of Animal Form*: University of Chicago Press.
Reinhardt, R., Centanin, L., Tavhelidse, T., Inoue, D., Wittbrodt, B., Concordet, J. P., Martinez-Morales, J. R. and Wittbrodt, J. (2015). Sox2, Tlx, Gli3, and Her9 converge on Rx2 to define retinal stem cells in vivo. *The EMBO Journal* **34**, 1572-1588.

Rembold, M., Loosli, F., Adams, R. J. and Wittbrodt, J. (2006). Individual cell migration serves as the driving force for optic vesicle evagination. *Science (New York, N.Y.)* **313**, 1130-1134.
Ruzicka, L., Howe, D. G., Ramachandran, S., Toro, S., Van Slyke, C. E., Bradford, Y. M., Eagle, A., Fashena, D., Frazer, K., Kalita, P., et al. (2019). The Zebrafish Information Network: new support for non-coding genes, richer Gene Ontology annotations and the Alliance of Genome Resources. *Nucleic Acids Res* **47**, D867-D873.
Saito, T., Goto-Kazeto, R., Fujimoto, T., Kawakami, Y., Arai, K. and Yamaha, E. (2010). Inter-species transplantation and migration of primordial germ cells in cyprinid fish. *Int J Dev Biol* **54**, 1481-1486.
Santos, F. V. (1929). Studies on Transplantation in Planaria. *The Biological Bulletin* **57**, 188-197.
---- (1931). Studies on Transplantation in Planaria. *Physiological Zoology* **4**, 111-164.
Sato, T., Vries, R. G., Snippert, H. J., van de Wetering, M., Barker, N., Stange, D. E., van Es, J. H., Abo, A., Kujala, P., Peters, P. J., et al. (2009). Single Lgr5 stem cells build crypt-villus structures in vitro without a mesenchymal niche. *Nature* **459**, 262-265.
Schaafhausen, M. K., Yang, W.-J., Centanin, L., Wittbrodt, J., Bosserhoff, A., Fischer, A., Schartl, M. and Meierjohann, S. (2013). Tumor angiogenesis is caused by single melanoma cells in a manner dependent on reactive oxygen species and NF-κB. *J Cell Sci* **126**, 3862-3872.
Schartl, M., Walter, R. B., Shen, Y., Garcia, T., Catchen, J., Amores, A., Braasch, I., Chalopin, D., Volff, J.-N., Lesch, K.-P., et al. (2013). The genome of the platyfish, Xiphophorus maculatus, provides insights into evolutionary adaptation and several complex traits. *Nature genetics* **45**, 567-572.
Schindelin, J., Arganda-Carreras, I., Frise, E., Kaynig, V., Longair, M., Pietzsch, T., Preibisch, S., Rueden, C., Saalfeld, S., Schmid, B., et al. (2012). Fiji: an open-source platform for biological-image analysis. *Nat Methods* **9**, 676-682.
Seleit, A., Krämer, I., Ambrosio, E., Dross, N., Engel, U. and Centanin, L. (2017). Sequential organogenesis sets two parallel sensory lines in medaka. *Development (Cambridge, England)* **144**, 687-697.
Soules, K. A. and Link, B. A. (2005). Morphogenesis of the anterior segment in the zebrafish eye. *BMC developmental biology* **5**, 12.
Souren, M., Martinez-Morales, J. R., Makri, P., Wittbrodt, B. and Wittbrodt, J. (2009). A global survey identifies novel upstream components of the Ath5 neurogenic network. *Genome biology* **10**, R92.
Spemann, H. and Mangold, H. (2001). Induction of embryonic primordia by implantation of organizers from a different species. 1923. *Int J Dev Biol* **45**, 13-38.
Storey, K. G., Crossley, J. M., De Robertis, E. M., Norris, W. E. and Stern, C. D. (1992). Neural induction and regionalisation in the chick embryo. *Development* **114**, 729-741.
Suga, H., Kadoshima, T., Minaguchi, M., Ohgushi, M., Soen, M., Nakano, T., Takata, N., Wataya, T., Muguruma, K., Miyoshi, H., et al. (2011). Self-formation of functional adenohypophysis in three-dimensional culture. *Nature* **480**, 57-62.
Rayon, T., D. Stamataki, R. Perez-Carrasco, L. Garcia-Perez, C. Barrington, M. Melchionda, K. Exelby, J. Lazaro, V. L. J. Tybulewicz, E. M. C. Fisher and J. Briscoe (2020). Species-specific pace of development is associated with differences in protein stability. Science **369** (6510), eaba7667

Trapnell, C., Roberts, A., Goff, L., Pertea, G., Kim, D., Kelley, D. R., Pimentel, H., Salzberg, S. L., Rinn, J. L. and Pachter, L. (2012). Differential gene and transcript expression analysis of RNA-seq experiments with TopHat and Cufflinks. *Nature protocols* **7**, 562-578.
Twitty, V. C. and Schwind, J. L. (1928). Growth of Heteroplastically Transplanted Eyes and Limbs in Amblystoma. *Proceedings of the Society for Experimental Biology and Medicine* **25**, 686-687.
---- (1931). The growth of eyes and limbs transplanted heteroplastically between two species of Amblystoma. *Journal of Experimental Zoology* **59**, 61-86.
van den Brink, S. C., Baillie-Johnson, P., Balayo, T., Hadjantonakis, A. K., Nowotschin, S., Turner, D. A. and Martinez Arias, A. (2014). Symmetry breaking, germ layer specification and axial organisation in aggregates of mouse embryonic stem cells. *Development* **141**, 4231-4242.

Vogeli, K. M., Jin, S.-W., Martin, G. R. and Stainier, D. Y. R. (2006). A common progenitor for haematopoietic and endothelial lineages in the zebrafish gastrula. *Nature* **443**, 337-339.
WADDINGTON, C. H. (1934). Experiments on Embryonic Induction. *Part I. The Competence of the Extra-Embryonic Ectoderm in the Chick* **11**, 212-217.
Wetts, R. and Fraser, S. E. (1988). Multipotent precursors can give rise to all major cell types of the frog retina. *Science* **239**, 1142-1145.
Winkler, S., Loosli, F., Henrich, T., Wakamatsu, Y. and Wittbrodt, J. (2000). The conditional medaka mutation eyeless uncouples patterning and morphogenesis of the eye. **127**, 1911-1919.
Wu, J., Greely, H. T., Jaenisch, R., Nakauchi, H., Rossant, J. and Belmonte, J. C. I. (2016). Stem cells and interspecies chimaeras. *Nature* **540**, 51-59.
Wu, J., Platero-Luengo, A., Sakurai, M., Sugawara, A., Gil, M. A., Yamauchi, T., Suzuki, K., Bogliotti, Y. S., Cuello, C., Morales Valencia, M., et al. (2017). Interspecies Chimerism with Mammalian Pluripotent Stem Cells. *Cell* **168**, 473-486.e415.
Yoda, H., Hirose, Y., Yasuoka, A., Sasado, T., Morinaga, C., Deguchi, T., Henrich, T., Iwanami, N., Watanabe, T., Osakada, M., et al. (2004). Mutations affecting retinotectal axonal pathfinding in Medaka, Oryzias latipes. *Mechanisms of development* **121**, 715-728.

Figures

Figure 1. Different developmental timing for zebrafish and medaka. Images of zebrafish (left) and medaka (right) embryos synchronised at the blastula stage (top, 512 cells, t = 0) and at different stages of embryonic development (hours post blastula, *hpb*). Eye cups (asterisks) are evident in zebrafish by 19*hpb*, retinal pigmentation (and neurogenesis) (arrows) by 26*hpb*, while in medaka it does not start before 48*hpb*. Scale Bars = 200 µm.

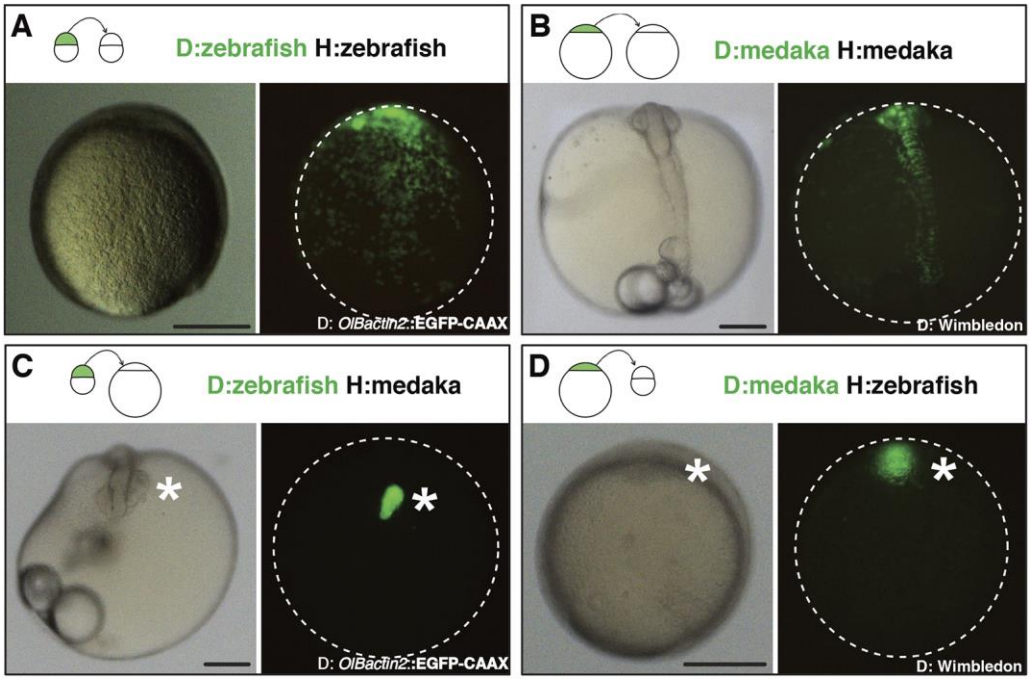

Figure 2. Intra and Inter-species transplantation of blastocysts in zebrafish and medaka. (A-D) Transmitted (left) and fluorescent (right) images of a non-labeled host embryo that was transplanted at a blastula stage with isochronic EGFP fluorescent cells. Images were taken after completion of initial morphogenesis (90% epiboly stage for zebrafish and early neurula stage for medaka), and transplantation schemes are displayed on top of each panel. Animal side is up for zebrafish hosts (A, D) and anterior side is up for medaka hosts (B, C). Dispersed green dots in A, B, are donor cells intermingled with host cells (N>20 transplantation events for each species, N>10 embryos per transplantation event. A *transplantation event* is a transplantation experiment performed on a given day with a specific donor-host combination, that lead to one or more chimeras of the described phenotype). EGFP+ clusters in C, D (asterisk) contain donor cells that did not mix with host cells. Representative images were chosen out of N = 10 zebraka and N = 12 medrafish. Clusters of the donor cells were found at later developmental stages in N = 17 transplantation experiments, N > 100 chimeras for zebraka; N = 33 transplantation experiments, N > 100 chimeras for medrafish (See Supplementary Tables 1 & 2). Scale Bars = 200 µm. D, donor; H, host.

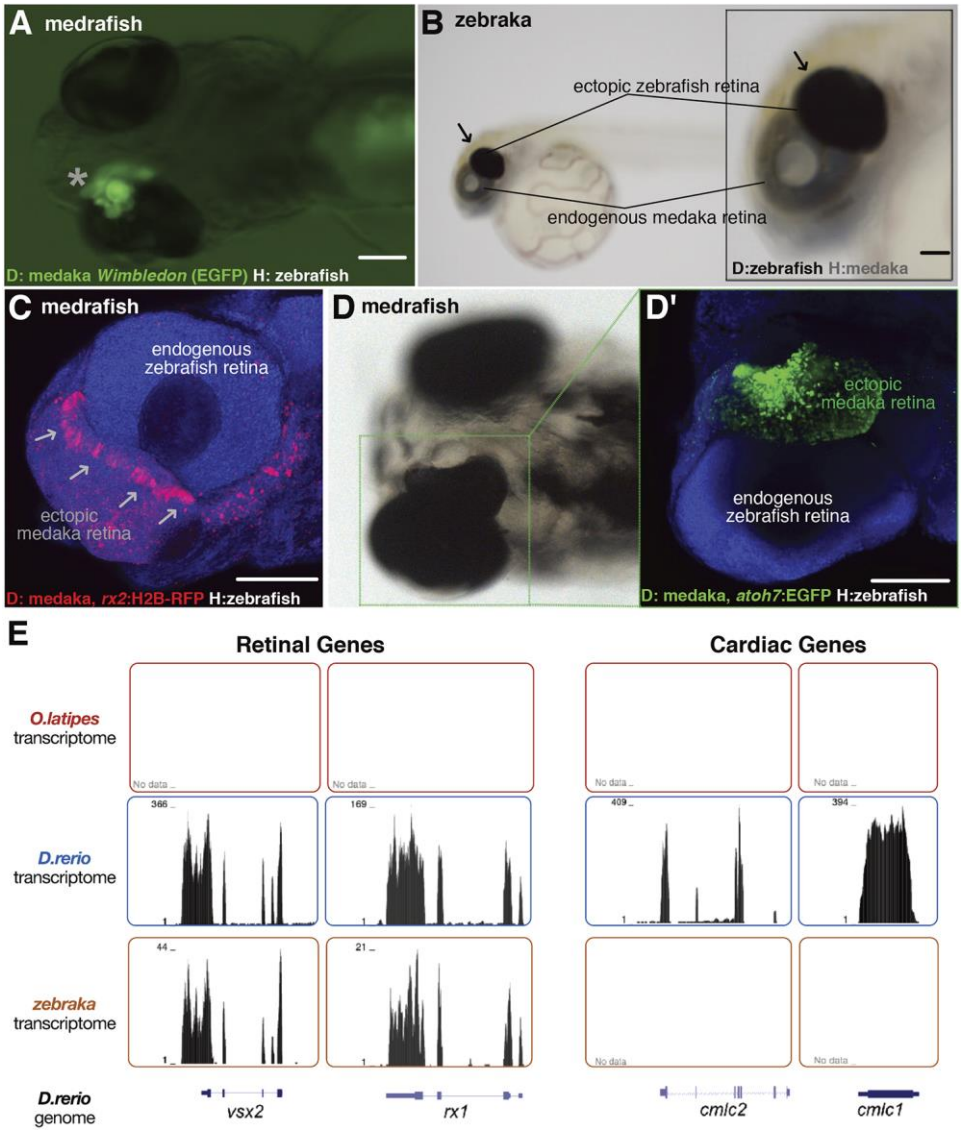

Figure 3. Transplanted EGFP+ cluster develops into an ectopic retina both in zebraka and medrafish. Images of medrafish **(A, C, D)** and zebraka **(B)**. The EGFP+ cluster (asterisk, ventral view of a hatch embryo, A) and the pigmented cluster (arrow, lateral view of a hatched embryo, B) develop into an ectopic retina (N = 45 transplantation events). Confocal images show expression markers of retinal progenitors (arrows in C, *Rx2*:H2B-RFP donors, medrafish at 4dpf) and retinal neurogenesis (D, *Atoh7*:EGFP donors, medrafish at 5dpf)(N = 17 transplantation events). **(E)** Transcriptomes of medaka (upper, N = 2), zebrafish (middle, N = 2) and zebraka (bottom, N = 3) plotted along the zebrafish genome. The zebrafish cells in medrafish display retinal identity (*vsx2, rx1*, left two panels) and no cardiac genes markers (*cmlc1&2*, right panels). Scale bars = 100 µm. D, donor; H, host.

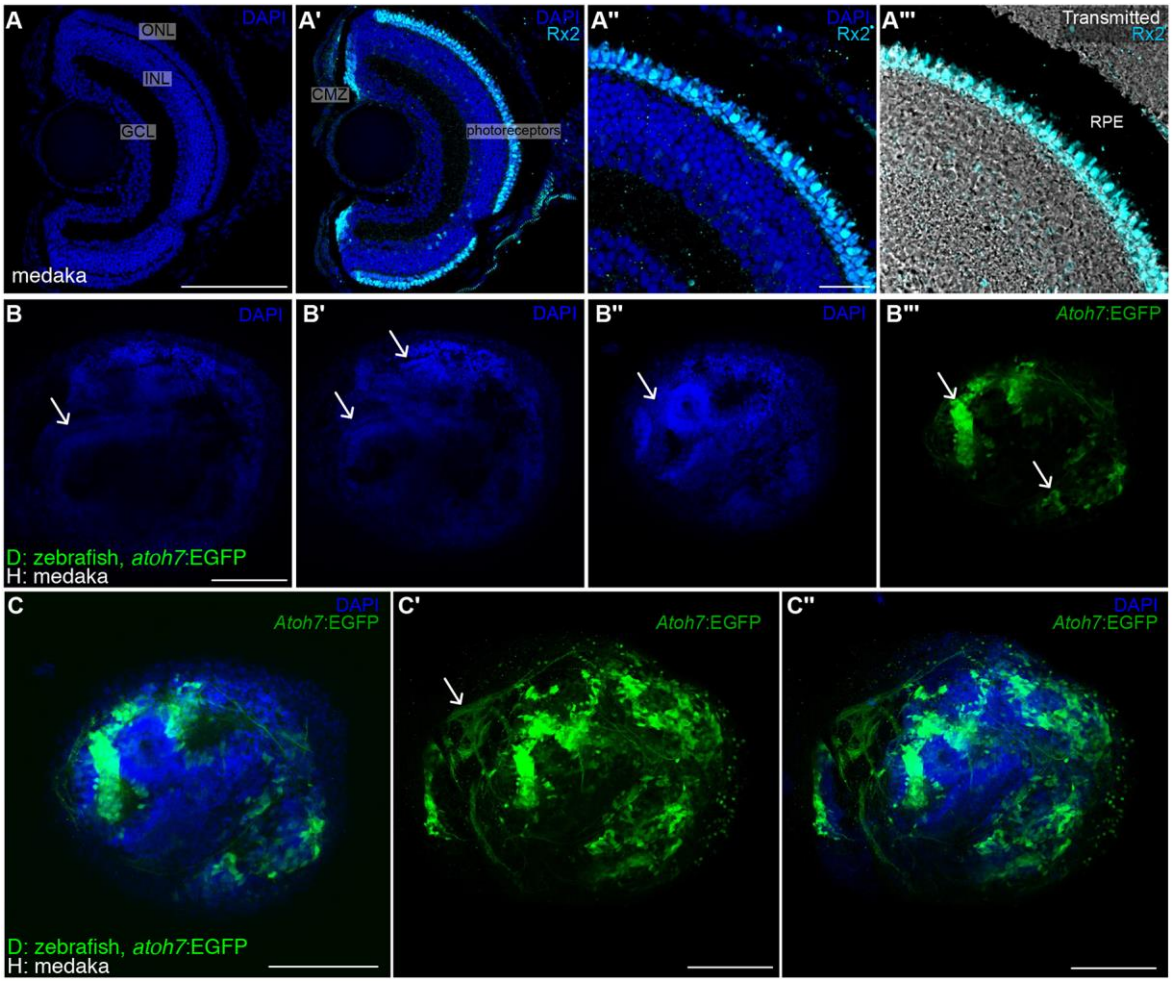

Figure 4. Topological organisation of retinal ganglion cells in ectopic retina. DAPI and immune-staining using an anti-Rx2 antibody on a medaka retina cryo-section **(A, A'')**. Retinal ganglion cells localise to the ganglion cell layer (GCL) and Rx2+ photoreceptors (Cyan staining in A'-A''') are found in the outer nuclear layer (ONL), adjacent to the retinal pigmented epithelium (black region in the transmitted channel, A'''). DAPI staining of whole mount retinae in zebrakas **(B-C'')** shows conspicuous layering (arrows in B, B') and clusters of retinal ganglion cells (arrows in B'', B''') labeled in green by using a Tg(*atoh7*:EGFP) zebrafish donor. Single plane (C) and stack (C',C'') showing RGCs and their axons (arrow in C') in an ectopic zebraka retina (N = 6 retinae in 6 chimeras). Scale bars = 100 µm, except for A'', A''' = 20 µm. GCL, ganglion cell layer; INL, inner cell layer; ONL, outer cell layer; CMZ, ciliary marginal zone; RPE, retinal pigmented epithelium; D, donor; H, host.

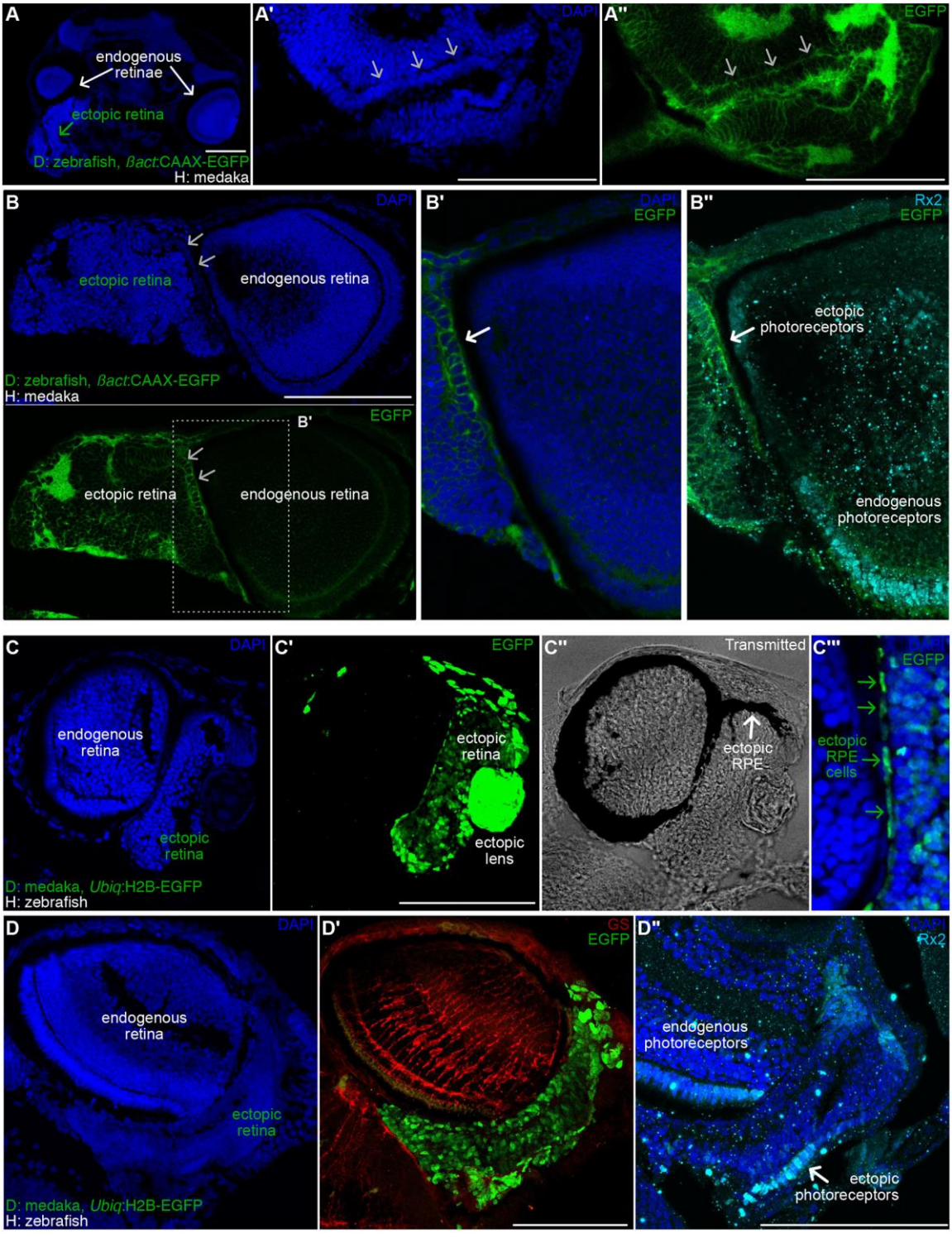

Figure 5. Partial layering in the ectopic retinae of zebraka and medrafish. DAPI staining on cryo-sections of zebrakas **(A, B'')** using Tg(*ßact*:CAAX-EGFP) zebrafish as donors. (A) Cryo-section of a transverse plane in a zebraka (dorsal is up, anterior is to the front), showing an ectopic retina (green arrow) ventrally adjacent to the endogenous retina (white arrow). Layering is evident in the ectopic retinae both by nuclear morphology (DAPI staining, arrows in A' and B, top) and by membrane accumulation (CAAX-EGFP, arrows in A'', B bottom and B') (N = 6 ectopic retinae in 6

zebrakas). Immuno-staining using anti-Rx2 Ab reveal photoreceptor identity of cells organised in layers (B'', white arrow) (N = 3 zebrakas). **(C, D'')** DAPI staining (C, D) on cryo-sections of medrafish using Tg(*Ubiq*:H2B-EGFP) medaka as donors. EGFP signal allows detecting ectopic cells (C', D'). Transmitted channel (C'') analysis reveals ectopic RPE covering the dorsal part of the ectopic retina (arrow). Merged channels (C'') showing co-localisation of elongated EGFP+ nuclei and pigmented epithelium (green arrows). Immuno-staining using an anti-GS antibody (D') reveals Muller glia in the endogenous retina and not in the ectopic retina (N = 4 medrafish). Immuno-staining using an anti-Rx2 antibody (D'') label ectopic photoreceptors (arrow) organised in a mononuclear layer (N = 3 medrafish). Scale bars = 100 µm. D, donor; H, host.

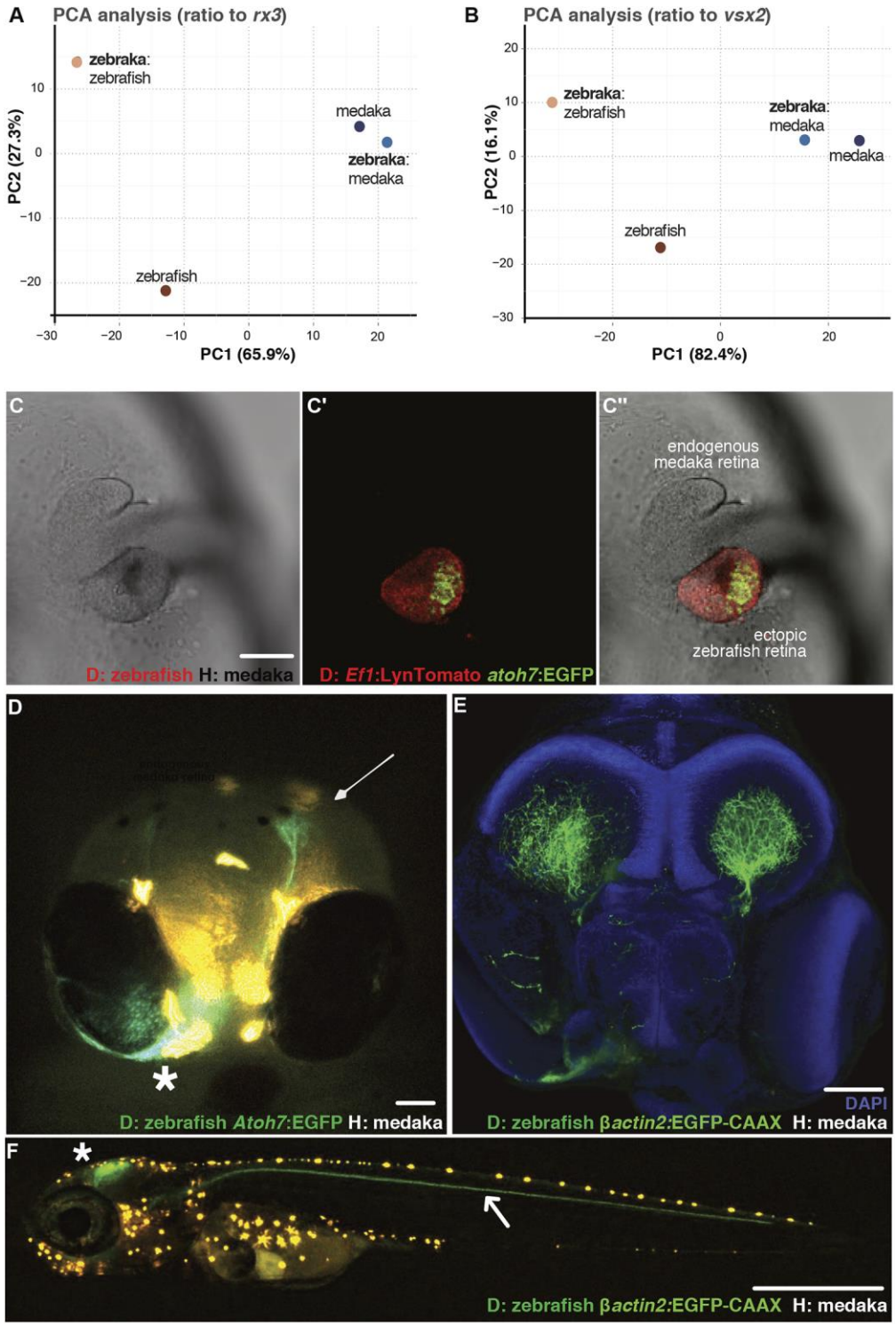

Figure 6. Retinogenesis follows a genetic developmental time. (A, B) PCA analysis of zebrafish and medaka orthologs expressed in the eye during the 24-48 hpf zebrafish developmental time window. The values are FPKM ratios between retinal genes and retinal progenitor markers *rx3* (A) and *vsx2* (B). **(C-C'')** Confocal images of the anterior region in a zebraka where the donor is Tg(*Ef1*:LynTomato, *atoh7*:EGFP) (C, transmitted; C' green and red channels; C'' merged image). EGFP expression in the transplanted cluster (C', C'') is evident at the vesicle stage of the medaka host (N= 3 chimeras). **(D)** Frontal view of a living 5dpf zebraka where the donor is Tg(*Ef1*:LynTomato,

atoh7:EGFP). Atoh7+ cells from the ectopic zebrafish retina (asterisk) migrate towards the endogenous medaka tectum (arrow) (N = 3 transplantation events, N= 6 chimeras). **(E)** Confocal image of a fixed 6 dpf zebraka where the donor is Tg(*Olßactin2*:EGFP-CAAX) ubiquitously labelling all donor cell projections (N = 2 transplantation events, N= 6 chimeras). Note that the ectopic retina projects to both host tecti. **(F)** Confocal image of a living zebraka at 9 dpf. A nerve coming from the ectopic zebrafish retina (located in the contralateral side) navigates along the posterior lateral line nerve (arrow). Other projections from the ectopic retina, presumably from later RGCs, project to the tectum (asterisk) (N = 4 transplantation events, N= 7 chimeras). Scale bars = 100 µm (C-E) and 1mm (F). D, donor; H, host. Orange dots in D and F correspond to medaka pigments.

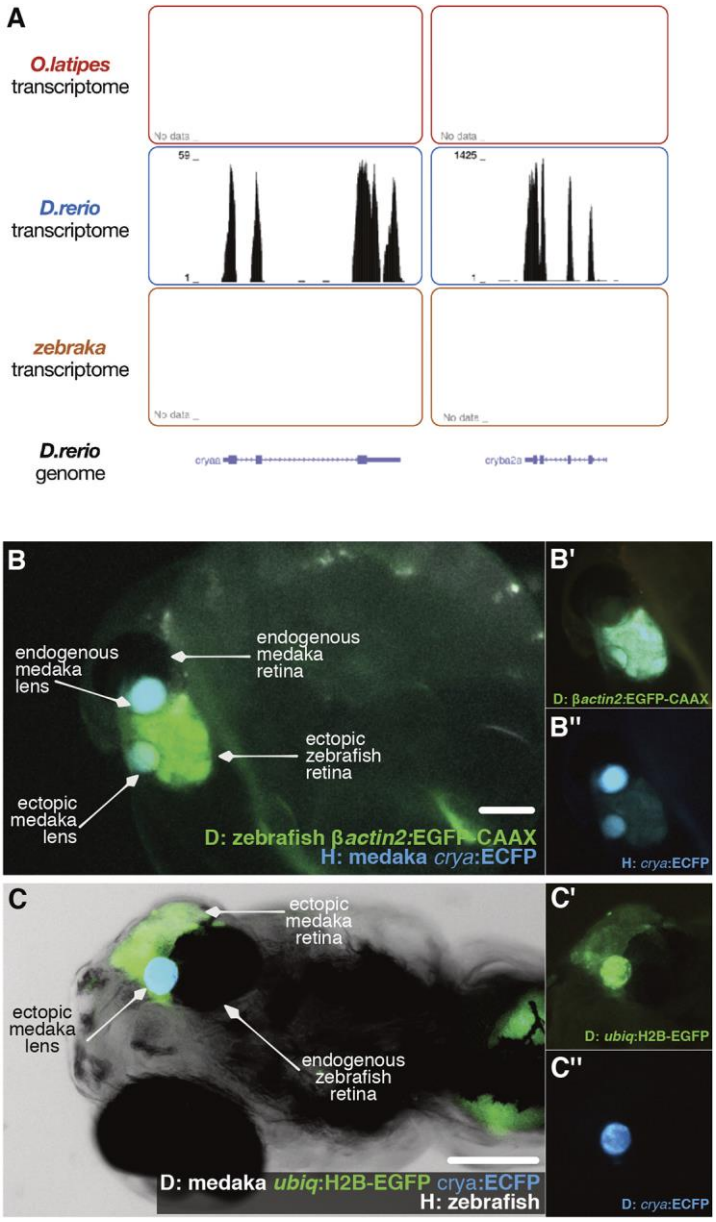

Figure 7. Ectopic zebrafish retina in zebrakas recruits the lens from the medaka host. (A) Transcriptomes of medaka (upper, N = 2), zebrafish (middle, N = 2) and zebraka (bottom, N = 3) plotted along the zebrafish genome. Lens zebrafish genes (*crystalin a* and *crystalin b a2a*, *cryaa* and *cryba2a* respectively) are expressed in zebrafish but not in zebrakas. **(B)** Lateral view of a zebraka where donor Tg(*OlBactin2*:CAAX-EGFP) cells were transplanted into a Tg(*crya*:ECFP) host. Merged (B) and single-channel images (EGFP in B', ECFP in B''). Cyan expression in the lens of the ectopic retina reveals its host origin (N = 3 transplantation events, N = 7 chimeras). **(C)** Ventral view of a medrafish at 5dpf, where donor Tg(*ubiq*:H2B-EGFP)(*crya*:ECFP) cells were transplanted into a non-labelled host. Merged (C) and single-channel images (EGFP in C', ECFP in C''). Cyan expression in the lens of the ectopic retina reveals its donor origin (N = 10 transplantation events, N = 23 chimeras). Scale bars = 100 µm. D, donor; H, host.

D: *D.r. Olßactin2*:EGFP **H:** *O.l*, Cab	Survival	Cluster formation	Ectopic retina	Notes
zebraka 1	**Y**	**Y**	**Y**	
zebraka 2	**N**			
zebraka 3	**Y**	**Y**	**Y**	
zebraka 4	**Y**	**Y**	**Y**	
zebraka 5	**Y**	**Y**	**Y**	
zebraka 6	**Y**	**Y**	**Y**	
zebraka 7	**Y**	**Y**	**Y**	

D: *D.r. Olßactin2*:EGFP **H:** *O.l*, LoxPOUT	Survival	Cluster formation	Ectopic retina	Notes
zebraka 8	**N**			
zebraka 9	**N**			
zebraka 10	**N**			
zebraka 11	**Y**	**N**	**N**	No GFP +

D: *D.r. Olßactin2*:EGFP **H:** *O.l*, GaudiRSG, *cmlc2*:ECFP	Survival	Cluster formation	Ectopic retina	Notes
zebraka 12	**Y**	**Y**	**Y**	
zebraka 13	**N**			
zebraka 14	**Y**	**Y**	**Y**	
zebraka 15	**Y**	**Y**	**Y**	
zebraka 16	**Y**	**N**	**N**	No GFP +
zebraka 17	**Y**	**N**	**N**	No GFP +

D: *D.r. Olßactin2*:EGFP **H:** *O.l*, *atoh7*:lyntdTomato	Survival	Cluster formation	Ectopic retina	Notes
zebraka 18	**Y**	**Y**	**Y**	
zebraka 19	**N**			
zebraka 20	**Y**	**Y**	**Y**	
zebraka 21	**Y**	**Y**	N/A	
zebraka 22	**N**			
zebraka 23	**N**			
zebraka 24	**Y**	**Y**	**Y**	
zebraka 25	**N**			

D: *D.r. atoh7:GFP, ef1:lynTomato* **H:** *O.l*, atoh7:lyntdTomato	Survival	Cluster formation	Ectopic retina	Notes
zebraka 26	**Y**	**Y**	**Y**	

D: *D.r. atoh7:GFP, ef1:lynTomato* **H:** *O.l*, Cab	Survival	Cluster formation	Ectopic retina	Notes
zebraka 27	**Y**	**Y**	**Y**	
zebraka 28	**Y**	**Y**	**Y**	
zebraka 29	**Y**	**Y**	**Y**	

D: *D.r. Olßactin2:lyntdTomato* **H:** *O.l*, *atoh7*:EGFP	Survival	Cluster formation	Ectopic retina	Notes
zebraka 30	**Y**	N/A	N/A	No Red +

Table S1. Zebraka transplantation experiments. List of transplantation experiments using zebrafish donor blastomeres to transplant into medaka blastulae. Genotypes of donor and hosts are indicated; each experiment is a different transplantation day (zebraka 1, zebraka 2, *etc*). Black cells represent cases in which no embryo survive beyond day 1; Y/N stands for Yes/No; N/A represents cases in which cluster formation or ectopic retina could not be assessed due to the lack of the reporter protein (typically, heterozygote donors)

D: *O.l.* LoxPout **H:** *D.r.* WIK/AB	Survival	Cluster formation	Ectopic retina	Notes
medrafish 1	**Y**	**Y**	**Y**	
medrafish 2	**Y**	**Y**	**N**	
medrafish 3	**Y**	**Y**	**Y**	
medrafish 4	**Y**	**Y**	**Y**	
medrafish 5	**Y**	**Y**	**N**	
medrafish 6	**Y**	**Y**	N/A	
medrafish 7	**Y**	**Y**	**Y**	
medrafish 8	**Y**	**Y**	**Y**	
medrafish 9	**Y**	**Y**	**Y**	
medrafish 10	**Y**	**Y**	**Y**	
medrafish 11	**Y**	**Y**	**Y**	
medrafish 12	**Y**	**Y**	**Y**	
medrafish 13	**Y**	**Y**	**Y**	

D: *O.l.* wimbledon **H:** *D.r.* WIK/AB	Survival	Cluster formation	Ectopic retina	Notes
medrafish 14	**Y**	**Y**	**Y**	

D: *O.l.* *fli*1:EGFP, *rx2*:H2B-mRFP **H:** *D.r.* WIK/AB	Survival	Cluster formation	Ectopic retina	Notes
medrafish 15	**Y**	**Y**	**Y**	
medrafish 16	**Y**	**Y**	**Y**	
medrafish 17	**Y**	**Y**	**Y**	
medrafish 18	**Y**	**Y**	N/A	
medrafish 19	**Y**	**Y**	**Y**	
medrafish 20	**Y**	N/A	N/A	No RFP +
medrafish 21	**Y**	N/A	N/A	No RFP +
medrafish 22	**Y**	N/A	N/A	No RFP +

D: *O.l.* *atoh7*:EGFP **H:** *D.r.* WIK/AB	Survival	Cluster formation	Ectopic retina	Notes
medrafish 23	**Y**	**Y**	**Y**	
medrafish 24	**Y**	**Y**	**Y**	
medrafish 25	**Y**	**Y**	**Y**	
medrafish 26	**Y**	**Y**	**Y**	
medrafish 27	**Y**	**Y**	**Y**	
medrafish 28	**Y**	**Y**	**Y**	
medrafish 29	**Y**	**Y**	**Y**	
medrafish 30	**Y**	**Y**	**Y**	
medrafish 31	**Y**	**Y**	**Y**	

D: *O.l.* *atoh7*:lyntdTomato **H:** *D.r.* WIK/AB	Survival	Cluster formation	Ectopic retina	Notes
medrafish 32	**Y**	N/A	N/A	No Red +
medrafish 33	**Y**	**Y**	**Y**	
medrafish 34	**Y**	**Y**	**Y**	
medrafish 35	**Y**	**Y**	**Y**	
medrafish 36	**Y**	**Y**	**Y**	
medrafish 37	**N**			
medrafish 38	**Y**	**Y**	**Y**	

Table S2. Medrafish transplantation experiments. List of transplantation experiments using medaka donor blastomeres to transplant into zebrafish blastulae. Genotypes of donor and hosts are indicated; each experiment is a different transplantation day (medrafish 1, medrafish 2, *etc*). Black cells represent cases in which no embryo survive beyond day 1; Y/N stands for Yes/No; N/A represents cases in which cluster formation or ectopic retina could not be assessed due to the lack of the reporter protein (typically, heterozygote donors)

		alignment vs OryLat2			alignment vs danRer10		
sample	*species*	*n reads tot*	*% alignment*	*n reads aligned*	*n reads tot*	*% alignment*	*n reads aligned*
1	medaka	52712186	**92,65 %**	48837840,3	52712186	**0,58 %**	305730,679
2	medaka	47861284	**88,28 %**	42251941,5	47861284	**0,52 %**	248878,677
3	zebrafish	65650278	**0,42 %**	275731,168	65650278	**90,45 %**	59380676,5
4	zebrafish	93625821	**0,37 %**	346415,538	93625821	**92,20 %**	86323007
5	zebraka	83057736	**88,08 %**	73157253,9	83057736	**2,24 %**	1860493,29
6	zebraka	65423949	**90,39 %**	59136707,5	65423949	**2,21 %**	1445869,27
7	zebraka	73869239	**88,06 %**	65049251,9	73869239	**2,24 %**	1654670,95

Table S3. Number of reads and alignment of transcriptomes to medaka and zebrafish genomes. Alignments of medaka, zebrafish and zebraka full transcriptomes to the genomes of medaka (version *OryLat2*) and zebrafish (version *danRer10*). Alignments are shown for each single transcriptome.

Organ	tracking_id	gene	medaka	zebrafish	zebraka
eye	ENSDARG00000002445	prdm1a	0	5,65089	4,94264
	ENSDARG00000003732	mitfa	0	5,50327	0,746289
	ENSDARG00000005574	vsx2	0	21,43285	103,344
	ENSDARG00000007480	rpe65a	0	2,077465	0
	ENSDARG00000014479	ptf1a	0	5,30958	21,0451
	ENSDARG00000039077	tyr	0	5,09426	2,16854
	ENSDARG00000040321	rx2	0	5,374545	21,0656
	ENSDARG00000052893	rx3	0	2,708445	2,24017
	ENSDARG00000054420	rpe65c	0	4,768605	0,741695
	ENSDARG00000056292	vsx1	0	6,713195	87,2205
	ENSDARG00000069552	atoh7	0	10,729815	164,963
	ENSDARG00000069737	pou4f2	0	2,10973	9,8081
	ENSDARG00000071684	rx1	0	9,31434	43,2672
	ENSDARG00000094752	rpe65b	0	27,16545	0,310149
	ENSDARG00000103379	pax6a	0	37,95835	284,621
	ENSDARG00000102047	mab21l1	0,803865	42,9119	136,364
	ENSDARG00000098925	prdm1b	0	5,21996	121,93
	ENSDARG00000019335	hes6	0	86,2615	194,179
	ENSDARG00000011235	otx2	0	20,428	152,552
	ENSDARG00000011989	crx	0	1,44177	41,3936
heart/muscle	ENSDARG00000032976	cmlc1	0	32,5024	0
	ENSDARG00000042018	fhl2a	0	6,662425	0
	ENSDARG00000098952	gata4	0	1,96555	0
	ENSDARG00000103589	gata6	0	14,02775	0
	ENSDARG00000037995	gdf3	0	0,612672	0
	ENSDARG00000099974	ldb3b	0	103,601	0
	ENSDARG00000035322	myh7bb	0	6,0762	0
	ENSDARG00000057317	nexn	0	27,1057	0
	ENSDARG00000005841	tnni2a.2	0	6,567225	0
	ENSDARG00000011400	tnnc1a	0	7,840665	0
	ENSDARG00000020610	tnnt2a	0	21,735	0
	ENSDARG00000029069	tnni2a.4	0	1569,055	0
	ENSDARG00000029995	tnni2b.2	0	19,1463	0
	ENSDARG00000035958	tnni2b.1	0	177,3585	0
	ENSDARG00000036671	tnni1al	0	93,67895	0
	ENSDARG00000042559	tnni1c	0	55,94625	0
	ENSDARG00000052708	tnni1b	0	17,72405	0
	ENSDARG00000002589	mylpfb	0	1381	0
	ENSDARG00000005629	smyd2b	0	20,64005	0
	ENSDARG00000007277	myf5	0	5,70612	0
	ENSDARG00000009133	myo1eb	0	11,5902	0
	ENSDARG00000011615	mybpc3	0	55,03795	0
	ENSDARG00000019096	myl7	0	30,3915	0
	ENSDARG00000021265	mybpc2b	0	54,02825	0
	ENSDARG00000061249	myom1a	0	58,81685	0
	ENSDARG00000062592	myl10	0	618,9045	0
	ENSDARG00000075433	myom2a	0	46,72825	0
	ENSDARG00000091099	myom2b	0	21,4495	0
	ENSDARG00000091253	smyd1b	0	24,88595	0
	ENSDARG00000099959	smyhc1	0,337096	168,427	0

Table S4. Transcriptional profile of ectopic cluster in zebrakas. List of zebrafish transcripts (and their ID) corresponding to retina genes (upper section) and heart genes (bottom section). The different columns show the count number of their respective sequences in transcriptomes from medaka, zebrafish and zebraka.

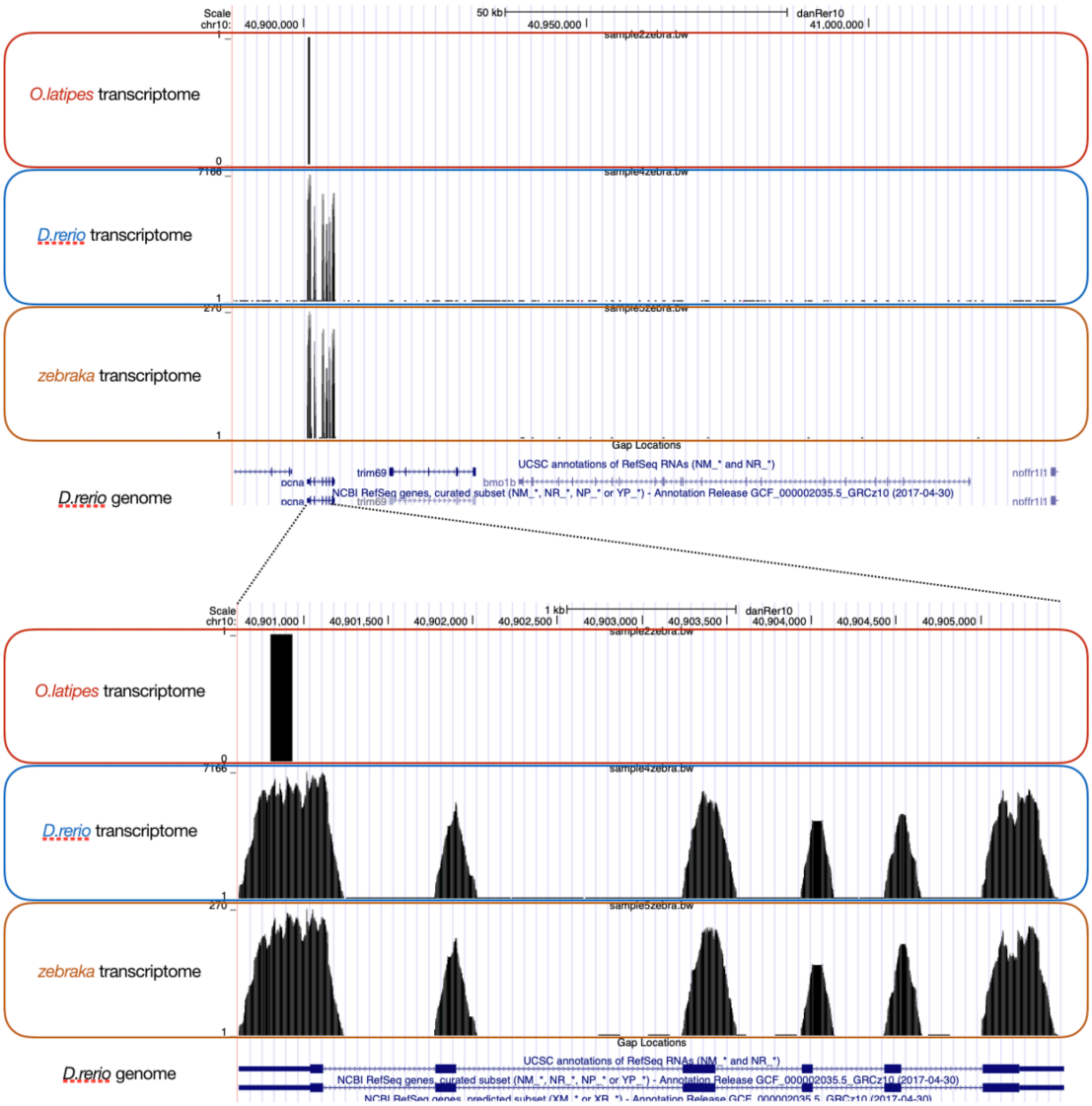

Supplementary Figure 1. Transcriptomes of medaka, zebrafish and zebraka plotted on the zebrafish genome

(Top) Transcriptomes from medaka are in the upper compartment, from zebrafish in the middle and from zebraka at the bottom. The image shows an example of a peak obtained using the medaka transcriptome. (Bottom) A detail of the region shows a different morphology for the medaka peak, different from the zebrafish or zebraka peaks that span along the entire set of exons of PCNA. Also note that the medaka peak consist of just one read, different from the >7K in zebrafish or >250 in zebraka.

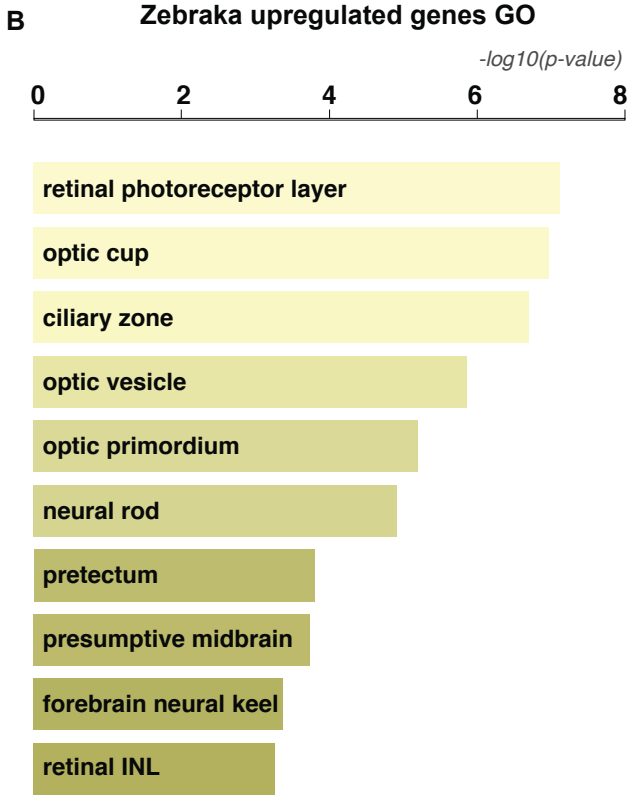

Supplementary Figure 2. Zebraka transcriptomic landscape at 48 hpf.

(A) Volcano plot illustrating the upregulated genes in the zebraka cells if compared with the zebrafish WT transcriptome. Each dot corresponds to a gene. Black dots indicate not significant variations; whereas red dots correspond to genes significantly upregulated in the zebraka cells (2434 genes). Grey dots indicate zebraka downregulated genes. (B) GO terms enriched in the zebraka upregulated genes ordered by significance.

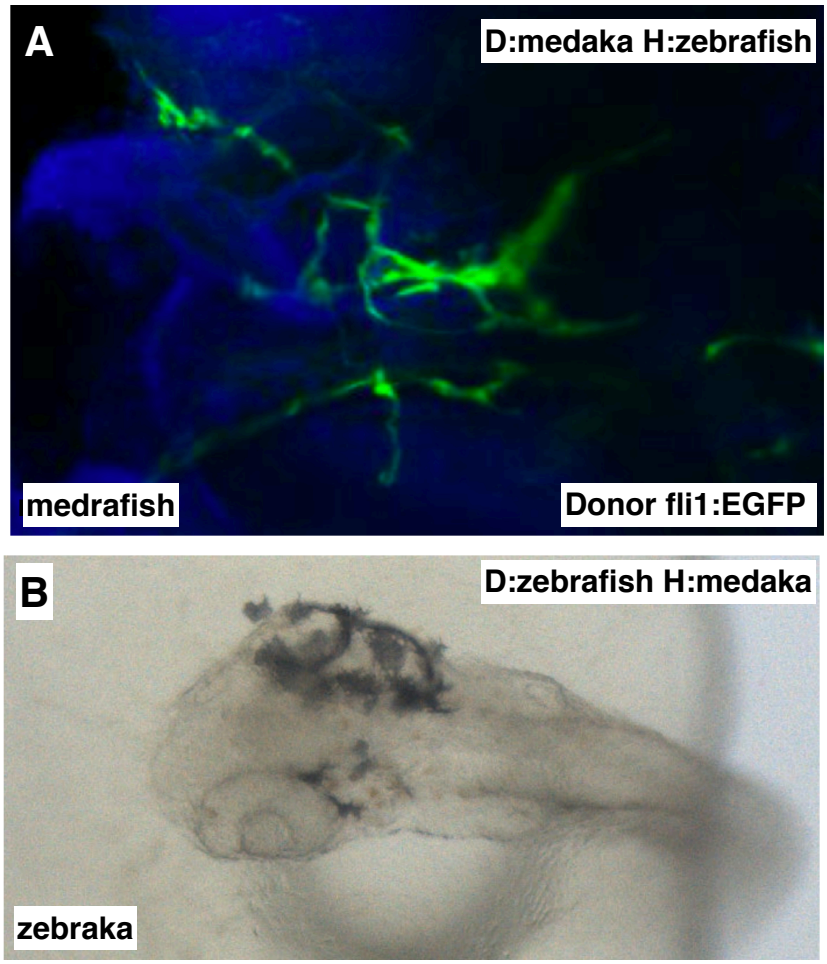

Supplementary Figure 3. Differentiation of donor cells in inter-species transplantations.

(A) Confocal image of 3 dpf medrafish using a Tg(fli1:EGFP) medaka donor (N = 3 transplantation events, N = 3 chimeras) (B) Binocular picture of a 2.5 dpf zebraka using a pigmented zebrafish donor and a wild type medaka host.

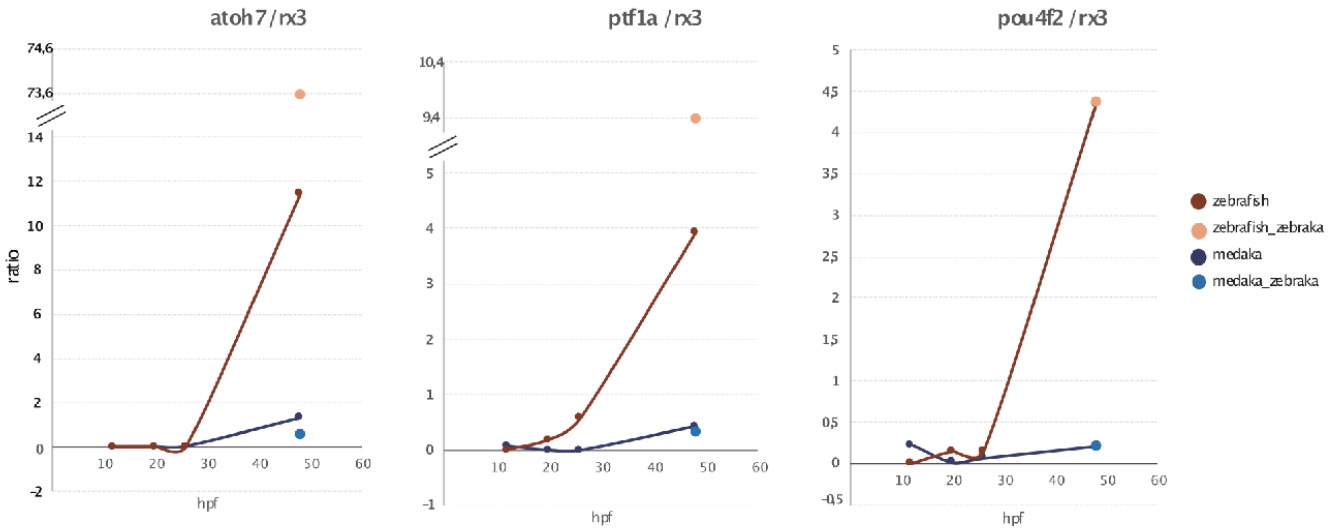

Supplementary Figure 4. Ratios of progenitor / differentiation retinal genes in zebrakas.

Plots show lines for the specified ratio during early embryonic development in zebrafish and medaka. The dots at 50hpf correspond to samples used in this study.

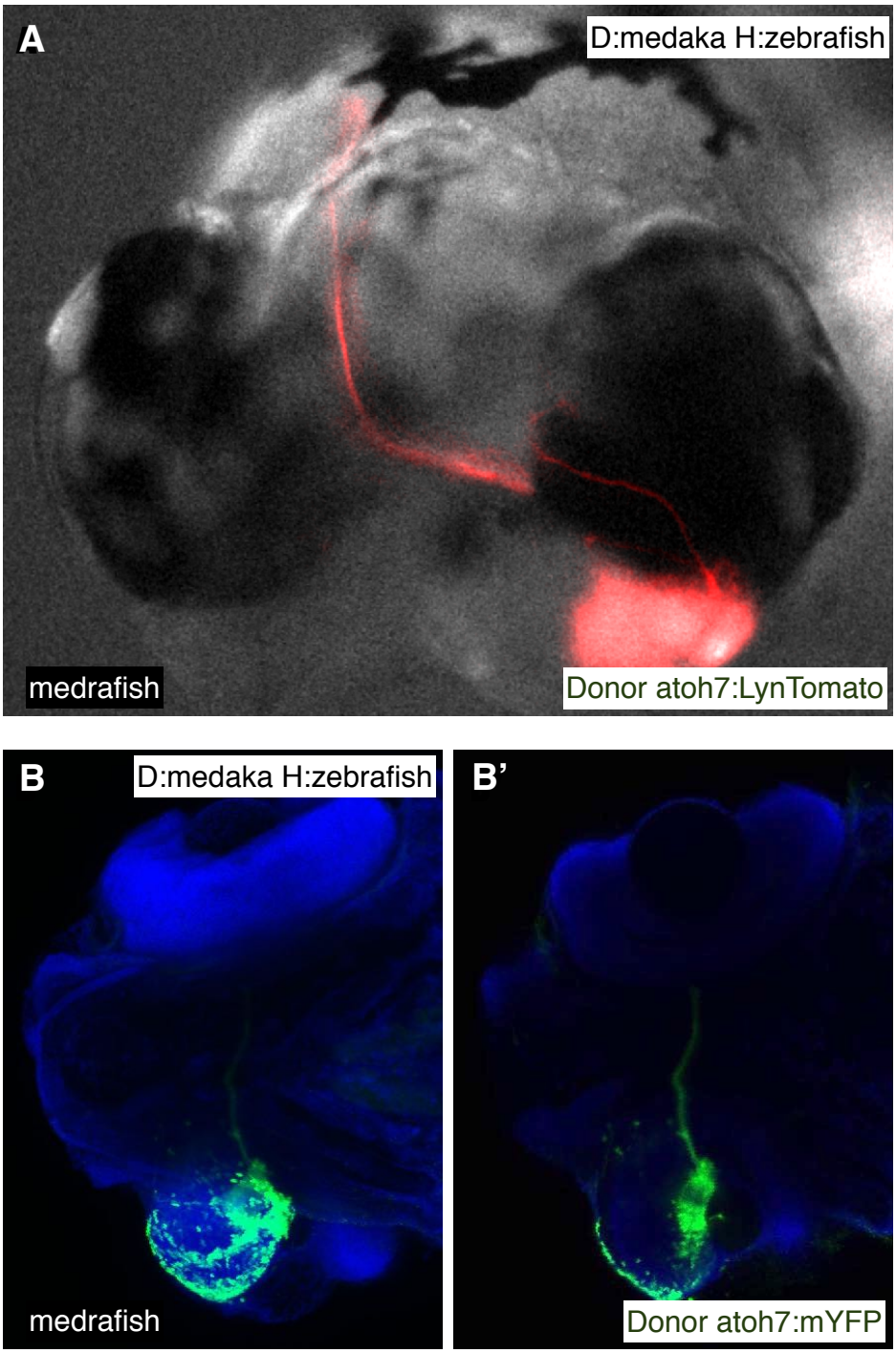

Supplementary Figure 5. Differentiation of RGCs is an ectopic medrafish retina.

(A, B) Confocal images of a 4 dpf medrafish using Tg(atoh7:LynTomato) (A) or Tg(atoh7:EGFP) (B) medaka donor and a non-transgenic zebrafish host. RGCs differentiate in the ectopic retina and form an optic nerve that projects to the host tectum. (A) Frontal view showing that axons of medaka RGCs travel to the contralateral host tectum (N = 2 chimeras) (B) Confocal section on medrafish ectopic retina showing EGFP+ RGCs. Deeper planes (B') show a proper organization of RGGs in the most inner layer (ganglion cell layer) and RGCs projections leaving the ectopic retina (N = 3 chimeras).

Supplementary Data S1

Click here to Download Data S1

Supplementary Data S2

Click here to Download Data S2